New Phytologist

Research

Exploring the metabolic basis of growth/defense trade-offs in complex environments with *Nicotiana attenuata* plants cosilenced in *NaMYC2a/b* expression

Caiqiong Yang, Yuechen Bai, Rayko Halitschke, Klaus Gase, Gundega Baldwin and Ian T. Baldwin

Department of Molecular Ecology, Max Planck Institute for Chemical Ecology, Hans-Knöll-Straße 8, Jena D-07745, Germany

Authors for correspondence:
Ian T. Baldwin
Email: baldwin@ice.mpg.de

Caiqiong Yang
Email: cyang@ice.mpg.de

Received: *10 October 2022*
Accepted: *3 January 2023*

New Phytologist (2023) **238:** 349–366
doi: 10.1111/nph.18732

Key words: competitor, field, glasshouse, mobile herbivores, specialized metabolites.

Summary

- In response to challenges from herbivores and competitors, plants use fitness-limiting resources to produce (auto)toxic defenses. Jasmonate signaling, mediated by MYC2 transcription factors (TF), is thought to reconfigure metabolism to minimize these formal costs of defense and optimize fitness in complex environments.
- To study the context-dependence of this metabolic reconfiguration, we cosilenced *NaMYC2a/b* by RNAi in *Nicotiana attenuata* and phenotyped plants in the field and increasingly realistic glasshouse setups with competitors and mobile herbivores.
- *NaMYC2a/b* had normal phytohormonal responses, and higher growth and fitness in herbivore-reduced environments, but were devastated in high herbivore-load environments in the field due to diminished accumulations of specialized metabolites. In setups with competitors and mobile herbivores, irMYC2a/b plants had lower fitness than empty vector (EV) in single-genotype setups but increased fitness in mixed-genotype setups. Correlational analyses of metabolic, resistance, and growth traits revealed the expected defense/growth associations for most sectors of primary and specialized metabolism. Notable exceptions were some HGL-DTGs and phenolamides that differed between single-genotype and mixed-genotype setups, consistent with expectations of a blurred functional trichotomy of metabolites.
- MYC2 TFs mediate the reconfiguration of primary and specialized metabolic sectors to allow plants to optimize their fitness in complex environments.

Introduction

Plants optimize resource use when attacked by herbivores to minimize fitness losses (McKey, 1974; Rhoades & Cates, 1976; Herms & Mattson, 1992); however, the mechanisms that regulate these physiological trade-offs are not well understood. Attack from chewing insects generally triggers a burst of jasmonate (JA) signaling in plants, a burst which is dramatically amplified when insect oral secretions (OS) are introduced into plant wounds during feeding, which, in turn, initiates defense metabolite synthesis and is accompanied by growth inhibition (Baldwin *et al.*, 1997; Baldwin & Hamilton, 2000; Heil & Baldwin, 2002; Halitschke & Baldwin, 2003; Kessler *et al.*, 2004; Stork *et al.*, 2009). As a consequence, apparent trade-offs occur between growth and defense.

Why the production of defenses is often associated with growth inhibitions remains unclear, but there are several theories that range from the architecture of the plant signaling systems that mediate growth/defense responses to fundamental characteristics of plant defenses. For example, many environmentally responsive plant hormones inhibit cell division or expansion (Pauwels *et al.*, 2008; Zhang & Turner, 2008; Noir *et al.*, 2013) and this arises primarily through cross-talk with other growth-controlling hormones such as auxin, brassinosteroids, and gibberellin (Chen *et al.*, 2011; Huot *et al.*, 2014). Jasmonate signaling, a common activator of defense, is also known to downregulate photosynthetic genes (Yadav *et al.*, 2005; Golovatskaya & Karnachuk, 2008), but photosynthetic capacity can be preserved during coronatine-induced JA signaling (Attaran *et al.*, 2014) and even increases during wound-induced alkaloid inductions (Baldwin & Ohnmeiss, 1994a). Plant defense production is known to command large fractions of whole-plant fitness-limiting (such as N) resources (Baldwin *et al.*, 1998; Bekaert *et al.*, 2012), some of which are nonrecyclable investments (Ohnmeiss & Baldwin, 1994). Moreover, defense metabolites can also be toxic for plants to produce (Baldwin & Callahan, 1993; Li *et al.*, 2021). This autotoxicity suggests that in competitive environments, a plant's metabolome may be influenced by its neighbors resulting in growth inhibitions, such as for terpenes released by plants attacked by chewing herbivores, which can decrease photosynthesis by 20% for 3 d (Gog *et al.*, 2005), morphological abnormalities, such as those associated with camptothecin accumulations in *Camptotheca* (Li *et al.*, 2010), or in the requirements for their biosynthesis in special tissues, compartmentalized storage or inactivation (Clay *et al.*, 2009; Erb & Kliebenstein, 2020). While

some signaling systems can be engineered to decouple growth-defense trade-offs, as demonstrated with the quintet JAZ and PHY B mutants in *Arabidopsis* (Campos *et al.*, 2016), it is clear that in most higher plants, JA signaling plays a central role in mediating the metabolic basis for this trade-off.

The regulatory functions of JA signaling are initiated by the binding of JA-isoleucine (JA-Ile) conjugates to CORONATINE INSENSITIVE 1 and the subsequent degradation of the jasmonate-Zim-Domain repressors (JAZs), which in turn, release the transcription factor (TF), MYC2, to activate the expression of downstream JA-responsive genes (Huot *et al.*, 2014; Pérez-Salamó *et al.*, 2019). In un-elicited conditions, JAZ proteins block MYC2's activity by recruiting the general corepressors TOPLESS (TPL) and TPL-related proteins, through an interaction with the adaptor protein, Novel Interactor of JAZ (Pauwels *et al.*, 2010; Wasternack & Kombrink, 2010).

MYC2 is a TF with a basic helix–loop–helix (bHLH) domain, that regulates the expression of several JA-responsive genes in both activating and repressive manners (Dombrecht *et al.*, 2007). These genes are mainly involved in growth, stress response, and specialized metabolic processes, including herbivore/pathogen defense (Schweizer *et al.*, 2013; Du *et al.*, 2017), drought tolerance (Wang *et al.*, 2020), circadian regulation (Shin *et al.*, 2012), photosynthesis, light signaling (Gupta *et al.*, 2014), seedling development (Srivastava *et al.*, 2019), and leaf senescence (Ding *et al.*, 2022). As a master regulator of JA signaling, MYC2 regulates the synthesis of most classes of specialized metabolites, including glucosinolate, nicotine, sesquiterpenoids, lactones, alkaloids, and phenolic acids, either directly or indirectly through other TFs (Schweizer *et al.*, 2013; Xu *et al.*, 2017; Sui *et al.*, 2018; Hayashi *et al.*, 2020; Huo *et al.*, 2021).

The specialized metabolites and their function have been thoroughly studied in *Nicotiana attenuata*, a native tobacco species of the Great Basin Desert of Utah, USA, which has been developed as an ecological model plant. *Nicotiana attenuata*'s defense against its specialist herbivore, *Manduca sexta*, has been extensively studied. Feeding by *M. sexta* larvae or applying its oral secretions and regurgitants (OS) to puncture wounds results in a burst of JAs (McCloud & Baldwin, 1997; Halitschke & Baldwin, 2004) and signals the *de novo* biosynthesis of many proven defense metabolites, such as nicotine (Steppuhn *et al.*, 2004; Kumar *et al.*, 2014), phenolamides (Kaur *et al.*, 2010; Gaquerel *et al.*, 2014) and phenolamine-GLV derivatives (Bai *et al.*, 2022), 17-hydroxygeranyllinalool diterpene glycosides (17-HGL-DTGs; Lou & Baldwin, 2003; Heiling *et al.*, 2010), and anti-digestive proteins (Zavala *et al.*, 2004; Kang *et al.*, 2006). When the MYC2-like TF (*NaMYC2a*) was silenced in *N. attenuata*, nicotine levels and the expression of phenolamide biosynthetic genes were decreased, but without affecting *M. sexta* larval performance or the accumulation of 17-HGL-DTGs (Woldemariam *et al.*, 2013).

Numerous studies have demonstrated plant growth/defense trade-offs with JA-signaling mutants (Bömer *et al.*, 2018; Oblessuc *et al.*, 2020) and exogenous JA treatments (Staswick *et al.*, 1992; Baldwin, 1998; Baldwin & Hamilton, 2000; Cao *et al.*, 2016), but the role of MYC2 as a master regulator of JA signaling in these trade-offs remains unclear. Here, we used RNA interference to cosilence *NaMYC2a* and *NaMYC2b* to explore these trade-offs in environments with herbivores and competitors, which are rarely included in studies of growth/defense trade-offs, despite their central roles as selective factors for plants (Kazan & Manners, 2013). To ensure that *NaMYC2a* and *NaMYC2b* cosilencing (irMYC2a/b) plants would be a suitable genetic tool for exploring these trade-offs, we first evaluated the performance of irMYC2a/b plants in the glasshouse and field in both high- and low-herbivore-load years. The herbivory-induced JA burst is both an important internal signal activating defense accumulations, and an important external signal used by some herbivores for host plant recognition (Kallenbach *et al.*, 2012) or detoxification of plant defenses (Li *et al.*, 2002). Moreover, as JAs are not only identified as a defense-related hormone but also involved in the regulation of important growth and developmental processes (Huang *et al.*, 2017), it was essential for our study of these trade-offs that the herbivory-induced phytohormonal responses remained intact while abrogating the JA-elicited responses.

We evaluated phytohormonal and metabolic responses to elicitations by wound and herbivore oral secretions (W + OS) treatments in both the glasshouse and the field. Cosilenced irMYC2a/b plants had normal OS-elicited JA bursts but had abrogated JA-induced primary and specialized metabolite responses. Since the cost of defense is not always obvious (Machado *et al.*, 2017), is often influenced by environmental factors such as intense competition and nutrient limitations (Cipollini *et al.*, 2017), and could be influenced by third-party trade-offs, such as with competitors (File *et al.*, 2012; Nerva *et al.*, 2022), we planted size-matched EV and irMYC2a/b plants in different combinations in 2 l pots, so that the EV or irMYC2a/b would be competing with isogenic neighbors. Plants were elicited with methyl jasmonate (MeJA) to ensure stable defense accumulation levels, profiled for metabolites, and a single neonate *M. sexta* larvae was placed on one of the two size-matched competing plants and allowed to move and feed freely for all but the penultimate instar. Larval movement between competing plants is an important and underappreciated aspect of induced defenses, as research with the *N. attenuata*–*M. sexta* system has demonstrated that the plant's powerful delayed inducible defenses allow the plant to use this herbivore as an offensive weapon against nearby competing plants (van Dam *et al.*, 2000; Stork *et al.*, 2009; Backmann *et al.*, 2019). To understand these complex interactions, data on larval movement, final larval mass, plant height, capsule number, plant dry mass, damaged leaves number, and capsule number per dry biomass of different competitive combinations were regressed against primary and specialized metabolite levels to infer metabolite functional roles in the growth/defense balance mediated by MYC2a/b TFs. The design and objectives of all the independent experiments in this study are summarized in Supporting Information Fig. S1.

Materials and Methods

Plant materials and growth conditions

Nicotiana attenuata Torr. Ex Watts seeds of the 31st generation inbred line originally collected at the DI ranch in southwestern

Utah, USA, were used as the wild-type (WT) genotype in all experiments. Seed germination and plant growth were performed as described previously (Krügel *et al.*, 2002); all glasshouse experiments were conducted with a day : night cycle of 16 h : 8 h, 26–28°C : 22–24°C in a glasshouse at the Max Planck Institute for Chemical Ecology, Jena, Germany.

For field experiments, the releases of the transformed plants were conducted under the Animal and Plant Health Inspection Service (APHIS) notification nos. AUTH-0000032827-22-02-13 (2020) and AUTH-0000089709-21-03-01 (2021) and transformed seeds were imported under permits 18-282-102m and 07-341-101n. Seeds were germinated on Gamborg's B5 medium and transferred to prehydrated 50-mm peat pellets 15 d after germination. Seedlings were watered and fertilized with iron solution (27.8 mg l^{-1} $FeSO_4 \cdot 7\ H_2O$ and 39.3 mg l^{-1} Titriplex® III in H_2O) every other day for 2 wk, after which the plants were transplanted into a field plot during two field seasons (2020 and 2021) and watered daily for *c.* 2 wk until the roots had established and plants were able to grow without water supplementation. Rosette diameters were measured every 6–10 d during the two field seasons.

MYC-like candidate identification and phylogenic analysis

The *N. attenuata* genome and protein sequences were downloaded through the Ensembl Plants database (http://plants.ensembl.org/info/data/ftp/index.html). The Hidden Markov Model (HMM) of the conservative structure domain of bHLH-MYC_N (PF14215) was downloaded from the Pfam database (https://www.ebi.ac.uk/interpro/) (Mistry *et al.*, 2020). Predicted MYC-like candidates were scanned with the Hmmer 3.0 software using the HMM file of the conserved domain of bHLH-MYC_N (Yang *et al.*, 2020). Protein sequences of MYC-like candidates (*E*-value < 0.001) were extracted with the TBtools v.1.09 software (Chen *et al.*, 2020). To ensure the accuracy of the results, the protein sequences of 25 candidates were submitted to the NCBI website (https://www.ncbi.nlm.nih.gov/Structure/cdd/wrpsb.cgi) for further verification. Sequence alignment and phylogeny reconstruction were performed on Mega 11 using ClustalW and neighbor-joining packages, respectively. The generated consensus tree was tested by bootstrapping (1000 times).

Plant transformation

Gene-specific 260-bp sequences of *NaMYC2a* (LOC109232914) and *NaMYC2b* (LOC109205493) were PCR amplified from *N. attenuata* UT-WT genomic DNA (gDNA), ligated by SalI sites, and inserted into the pSOL8DCL2 transformation vector (GenBank no. HQ698851), yielding pSOL8MYC2a/b. PCR was performed using Phusion High-Fidelity DNA Polymerase (Thermo Fisher Scientific; www.thermofisher.com). gDNA was isolated by a modified cetyltrimethylammonium bromide method (Bubner *et al.*, 2004). *Nicotiana attenuata* plants (UT-WT 31st inbred generation) were transformed with pSOL8-MYC2a/b T-DNA using *Agrobacterium tumefaciens* LBA4404 with the transformation method described in Krügel *et al.* (2002). Homozygous transgenic lines with single T-DNA insertions were selected by screening T_2 and T_3 generation seedlings that showed hygromycin resistance in the expected segregation ratios. The completeness of the T-DNA integrations into the plant genome was confirmed by diagnostic PCRs with the respective gDNA as template. Real-time qPCR (RT-qPCR) was used to select the best silenced transgenic lines. All sequences of the primers used for gene amplification, cloning, diagnostic PCRs, and RT-qPCR were given in Table S1.

Metabolite elicitations in field and glasshouse

The first stem leaves were treated with wounding and *M. sexta* oral secretions (W + OS) both in the field (2021) and glasshouse, and leaves were wounded with three rows of puncture wounds on each side of the midrib with a fabric pattern wheel and immediately treated with 20 µl of 1 : 5 diluted *M. sexta* oral secretions; plants treated with matched W + water treatments were used as controls in glasshouse experiments; unwounded plants were used as controls for elicitations in the field (McCloud & Baldwin, 1997; Halitschke *et al.*, 2001). Samples were collected at 0, 1, and 48 h, and all samples were immediately frozen on dry ice (field) or in liquid nitrogen (glasshouse). The collected samples were stored at −80°C for quantification of phytohormones, primary, and specialized metabolites. For MeJA treatments, lanolin with 250 µg MeJA was applied to the adaxial surface of the first stem leaves, and plants treated similarly with pure lanolin were used as a control (Baldwin, 1996). Samples were collected after 72 h, immediately frozen in liquid nitrogen, and stored at −80°C for untargeted metabonomics analysis.

Insect performance assay of noncompetitive plants

Manduca sexta performance assays with singly grown plant were conducted on stably transformed lines in the glasshouse as described previously (Pradhan *et al.*, 2017; Heiling *et al.*, 2021) with 15 replicate plants per treatment. Glasshouse plants were grown in a completely randomized design. Neonates were placed on the abaxial surface of the second fully developed leaf of rosette-stage plants. Larvae were allowed to feed for 11–13 d; larval mass was recorded every 2–3 d.

Competitive experiment

Limited resources will amplify the impact of defense production on plant growth. In order to study the impact of silencing *NaMYC2a/b* on the growth-defense trade-off and evaluate whether this trade-off is influenced by third-party factors, we conducted a competitive experiment in the glasshouse as described in the timeline shown in Fig. S2. Two size-matched EV (E) or irMYC2a/b (M) seedlings were planted in different combinations in a single 2 l pot in the glasshouse, as single (EE, M1M1, and M1M2) and mixed-genotype (EM1, EM2, M1E, and M2E) combinations. Seven days after seedling transfer, both plants in the pot were elicited with 250 µg of MeJA in 20 µl lanolin, applied to the adaxial surface of two leaves (Baldwin, 1996)

for 72 h to ensure that the defense system of plants were fully elicited; one of the treated leaves was harvested for metabolite analysis at 72 h to elucidate metabolic profile differences in EV and irMYC2a/b under the single and mixed combination. A freshly eclosed *M. sexta* neonate larvae were placed on the left of two competing plants (plants labeled A), either an EV (E) or irMYC2a/b (M) plant depending on the genotype treatment group (EE, MM, EM, or ME). The larvae were allowed to feed and move freely without any additional touching or disturbance. Normally, larvae do not move from the leaf on which they were 'oviposited' for at least 2–3 d of feeding. Hence, we categorized treatments as representing 'high defense' (EE), 'weak defense' (M1M1 and M2M2), and 'priority defense' (EM1, EM2) or 'delayed defense' (M1E, M2E) treatments for these larvae that were fully capable of moving between plants in a pot as they transitioned into the second instar. We recorded the location of the caterpillar and the plant height every 2–3 d as indicated in the timeline of Fig. S2. After the caterpillars reached the fifth instar, the mass of each caterpillar was recorded. When the plants were mature, the number of damaged leaves, the final capsule number, and fresh and dry biomass of the plants were quantified.

Metabolite extraction and analysis

Extraction and chromatographic analysis procedures of primary and specialized metabolites were based on previously published methods (Gaquerel *et al.*, 2010; Schäfer *et al.*, 2016) with small modifications (Methods S1).

Metabolomics analysis

Raw data files were converted into netCDF format and preprocessed with R packages XCMS and CAMERA using the following parameters: centWave method; ppm = 20; snthresh = 10; peak width = between 5 and 18 s; minfrac = 0.5; minsamp = 1; bw = 10; mzwid = 0.01; sleep = 0.001. The FillPeaks function from XCMS was used to fill missing features. The output data file was submitted to METABOANALYST 5.0 for principal component analyses (PCA) and partial least squares discriminant analyses (PLS-DA). Log transformation (Base 10) and Pareto Scaling (mean-centered and divided by the square root of the standard deviation) were used for sample normalization before the analysis. The significant MS features were obtained by PLS-DA with the variable importance in projection (VIP-value) > 1 and submitted to VENNY v.2.0 https://bioinfogp.cnb.csic.es/tools/venny/ to obtain candidate features for irMYC2a/b regulation. KEGG pathway analysis of candidate features was performed by METABOANALYST v.5.0 (MS peak Function Analysis).

Transcriptome sequencing and transcript abundance analysis

Total RNA was isolated from rosette leaves of *N. attenuata* using the plant RNA Purification Kit (Macherey-Nagel, Düren, Germany) according to the manufacturer's instructions. Transcriptome sequencing analysis was performed by the Novogene Co. (https://www.novogene.com/). In brief, the total RNA of W + OS-induced WT and irMYC2a/b leaves were used to construct the strand-specific RNA libraries. Sequencing was performed on an Illumina HiSeq platform (Illumina HiSeq™ 2500; Illumina, San Diego, CA, USA), and gene annotation was based on the genome of *N. attenuata* (Assembly NIATTr2). RT-qPCR was performed on a Stratagene Mx3005P qPCR machine using a Takyon™ No ROX SYBR 2X MasterMix Blue dTTP (Eurogentec, Seraing, Belgium). *Nicotiana attenuata* housekeeping gene *IF-5A* was used as an internal reference. Primer sequences are listed in Table S1.

Statistical analysis

Statistical analysis of the data was performed using GRAPHPAD PRISM 9.2 (GraphPad Software, La Jolla, CA, USA) and IBM SPSS STATISTICS 23 (SPSS, v.20.0; IBM Inc., Chicago, IL, USA). Data were evaluated using analysis of variance (ANOVA), followed by Tukey's honestly significant difference and two-tailed Student *t*-tests. Heatmap and correlation analyses were performed using R packages COMPLEXHEATMAP, CORRPLOT, and PSYCH.

Gene annotation number

NaMYC2a (LOC109232914), *NaMYC2b* (LOC109205493), *NaGGPPS* (LOC109210081), *NaGLS* (LOC109243172), *NaAT1* (LOC109237700), *NaDH29* (LOC109206371), *NaCV28* (LOC109206370), *NaPAL* (LOC109212354), and *NaC4H* (LOC109215399).

Results

Cosilencing *NaMYC2a/b* robustly increased growth at the expense of herbivore resistance

A *N. attenuata*-specific HMM for the bHLH-MYC_N (PF14215) domain (Pattanaik *et al.*, 2008) was used to identify MYC-like TFs, from which a total 25 of nonredundant MYC-like candidates were identified in the *N. attenuata* genome. The candidate protein sequences were compared with the reported MYC2 protein sequences of *Arabidopsis thaliana* (*AtMYC2* AT1G32640) (Zhang *et al.*, 2018) and tomato (*SlMYC2* Solyc08g076930) (Du *et al.*, 2017) by phylogenic analysis to identify possible *N. attenuata* MYC2s. Phylogenic analysis indicated that *NaMYC2a*, *NaMYC2b*, and *NaMYC2_2* were in the same clade as *AtMYC2* and *SlMYC2* (Fig. S3a). The transcript abundances of *NaMYC2a* and *NaMYC2b*, but not *NaMYC2_2*, were strongly increased in response to W + OS treatment (Fig. S3b); thus, *NaMYC2a* and *NaMYC2b* were used for all subsequent experiments. Gene-specific 260-bp sequences of *NaMYC2a* and *NaMYC2b* were cloned, ligated with SalI sites, and inserted into a pSOL8 vector to transform the 31st inbred generation of UT-WT *N. attenuata* to generate homozygous single-insertion transgenic lines cosilenced in *NaMYC2a* and *NaMYC2b* expression (Figs S3c, S4a,b). The silencing efficiency of *NaMYC2a* in three independently transformed lines A-17-108-1-1, A-17-110-2-1, and A-17-

111-6-2 were 62%, 61%, and 70%, respectively, and that of *NaMYC2b* were 83%, 81%, and 79%, respectively (Fig. S4c). Transformed lines A-17-108-1-1 (irMYC2a/b#1) and A-17-110-2-1 (irMYC2a/b#2) were used in all subsequent experiments.

The *NaMYC2a* and *NaMYC2b* cosilenced plants (irMYC2a/b) had robustly faster growth rates at the expense of herbivore resistance compared with EV plants. In individually grown plants in the glasshouse, irMYC2a/b seedling length (Fig. 1a), rosette diameter (Fig. 1b), and flowering stalk heights (Fig. 1c) were 77.3–92.1%, 38.2%, and 10.0–19.6%, respectively, greater than those of EV plants. Additionally, flowers of irMYC2a/b plants had reduced corolla lengths by 13.2–20.1% (Fig. 1d). In these non-competitive, single plant/pot conditions, capsule production rates were initially higher, consistent with the higher vegetative growth rates of irMYC2a/b plants, but no differences were observed in the final capsule numbers between EV and irMYC2a/b plants (Fig. 1e). In the glasshouse, larvae fed on irMYC2a/b were on average 3.3–3.7 times larger than those feeding on EV (Fig. 1f).

Initially, size-matched seedlings were planted into a field plot in the plant's native habitat in the Great Basin Desert, over two field seasons that differed dramatically in natural herbivore loads. During the low-herbivore abundance year (2021), irMYC2a/b

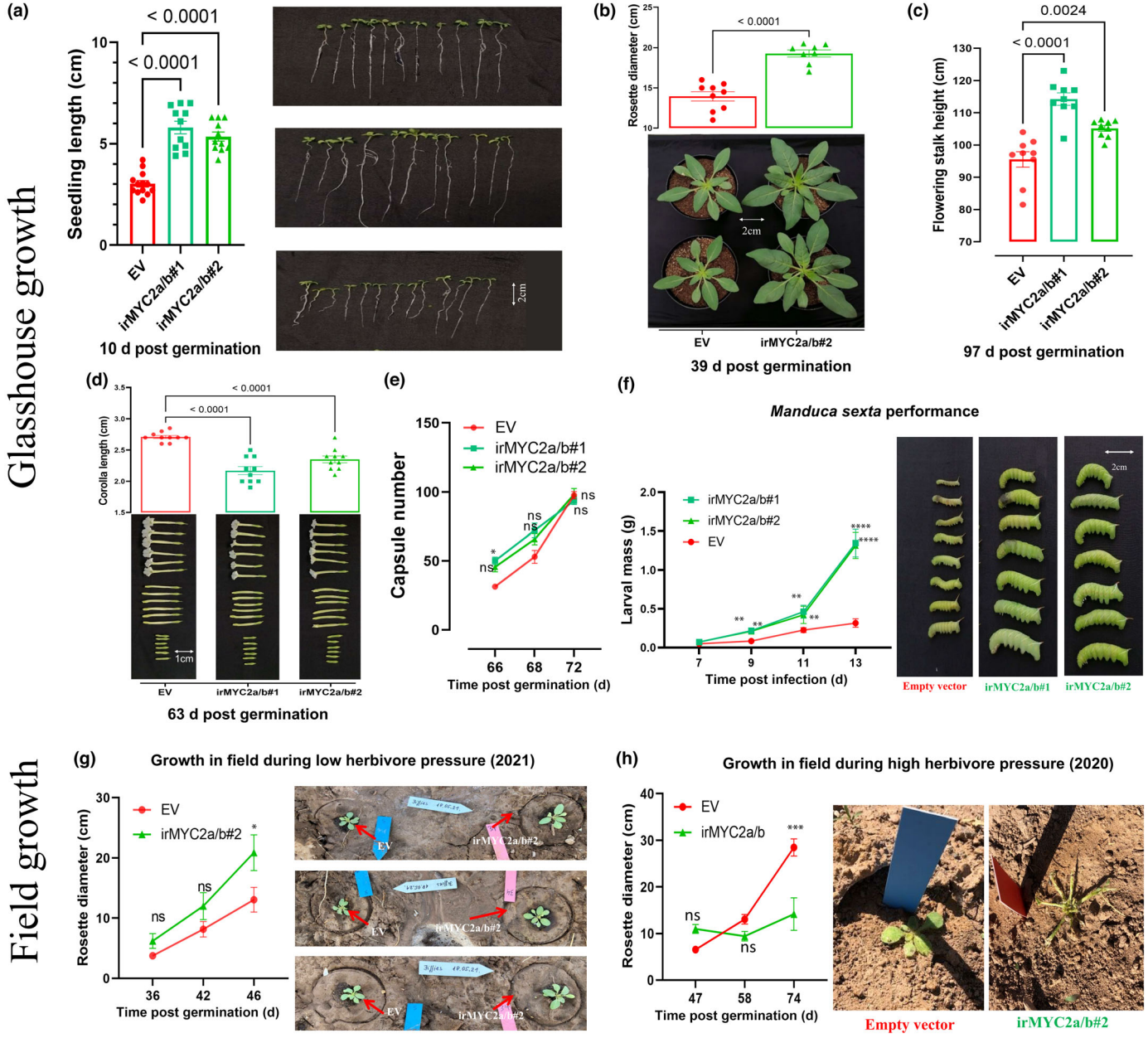

Fig. 1 Growth and defense phenotypes in the glasshouse (a–f) and field (g, h). (a) Seedling length ($n = 12$–15); (b) rosette diameter ($n = 9$); (c) flowering stalk heights ($n = 10$); (d) corolla length ($n = 10$); (e) capsule number ($n = 10$); (f) weight of *Manduca sexta* larvae ($n = 15$); (g) rosette diameter in 2021; (h) herbivore damage and rosette diameter in 2020 ($n = 12$–20) of two independent lines of *MYC2a/b* cosilenced (irMYC2a/b#1 and #2) and empty vector (EV) control plants. Results of ANOVAs and Tukey's test, and two-tailed Student's *t*-test are shown (mean ± SE; *, $P < 0.05$; **, $P < 0.01$; ***, $P < 0.001$; ****, $P < 0.0001$; ns, not significant). Red circles, EV plants; dark green squares, irMYC2a/b#1 plants; green triangles, irMYC2a/b#2 plants.

plants showed the same growth advantage over EV (Fig. 1g) as observed in the glasshouse. However, in the 2020 field season of high herbivore loads (damage by cutworms, grasshoppers, and tree crickets), irMYC2a/b plants were continuously damaged and without daily insecticide spraying and manual insect removals, none would have survived to the flowering stage (Fig. 1h).

OS-elicited phytohormonal bursts are unaltered in irMYC2a/b plants in glasshouse and field

MYC2 is a positive regulator of the JA-signaling pathway (Kazan & Manners, 2013), participates in a feedback loop with the biosynthesis of jasmonic acid in Arabidopsis, and controls genes involved in the production of phytohormones (Dombrecht *et al.*, 2007). However, in *N. attenuata*, no consistent differences were observed between EV and irMYC2a/b plants in their OS-elicited phytohormone levels, for JA, JA-Ile, OH-JA-Ile, SA, or ABA in either glasshouse- (Fig. 2a) or field-grown (Fig. 2b) plants during the low-herbivore-load field season of 2021. During the 2020 field season, irMYC2a/b plants had no undamaged leaves with which to conduct OS-elicitation experiments.

Silencing MYC2a/b dramatically alters basal and OS-elicited levels of primary and specialized metabolites

The metabolic responses of irMYC2a/b and EV plants to OS elicitation were analyzed in the field- (Fig. S5) and in glasshouse-grown plants (Fig. 3) to evaluate their utility for the analysis of growth/defense trade-offs. After 72 h, W + OS treatment of EV decreased the concentrations of Chl*a* and Chl*b*, by 47.3% and 33.8% (Fig. 3a) and glucose, sucrose, fructose, and cellobiose, by 76.7%, 52.9%, 60.8%, and 63.1%, respectively (Fig. 3a). By contrast, these reductions were completely abolished in irMYC2a/b plants (Fig. 3a). Additionally, independent of W + OS elicitation, irMYC2a/b had higher amino acid levels (Fig. 3b). By contrast, irMYC2a/b plants had decreased acyl sugar levels (O-AS) both in the glasshouse (Fig. 3c), and field (Fig. S5). O-AS#9 was not detectable in irMYC2a/b plants and the other O-AS were decreased by 46.3–92.3% in irMYC2a/b compared with EV plants (Fig. 3c). Nicotine levels in irMYC2a/b decreased by 95.6 (irMYC2a/b#1) to 96.7% (irMYC2a/b#2) compared with EV plants (Fig. 3c). For the inducible defense compounds, phenolamides and HGL-DTGs, cosilencing of *NaMYC2a/b* significantly reduced transcript levels of key genes involved in phenolamide and HGL-DTG biosynthesis. The transcript levels of *NaPAL1*, *NaC4H*, *NaAT1*, *NaDH29*, and *NaCV86* in irMYC2a/b plants were only 0.60–9.09% of those in EV plants (Fig. 3c). Similarly, the accumulation of phenolamides was also significantly decreased and most compounds were not detected in irMYC2a/b plants. The induction of phenolamides, such as *N*-caffeoylputrescine (CP), *N*′,*N*″-di-caffeoylspermidine (DCS), coumaroylputrescine (COP), feruloylputrescine (FP), and monohydrated *N*′,*N*″-di-caffeoyl spermidine (MDCS), was almost completely abolished in irMYC2a/b plants (Figs 3c, S5). Although cosilencing *NaMYC2a/b* significantly decreased the transcript levels for key genes involved in the synthesis of HGL-DTGs (*NaGGPPS* decreased by 72.3–61.5%; *NaGLS* by 95.3–88.5%; Fig. 3c), the two most abundant HGL-DTGs, lyciumoside I and nicotianoside II, were significantly increased in irMYC2a/b control plants and were decreased after W + OS elicitation (Fig. 3c).

Competitive growth affects the MeJA-elicited responses of EV and irMYC2a/b plants differently

Principal component analysis plots of the metabolomes of EV plants grown without competitors revealed complete separations of metabolomes in response to MeJA elicitation on the first two principal components (PC1, accounting for 22%, and PC2, accounting for 13% of the total variance). The control and elicited metabolomes of irMYC2a/b plants largely overlapped, but were completely separated from those of EV plants on PC1 (Fig. 4a). This suggests that *NaMYC2a/b* silencing dramatically alters the basal metabolic profiles and abolishes the response to MeJA elicitation. In total, 454 and 383 differential MS features were obtained from control and MeJA-elicited plants, respectively, with 203 of these MS features being shared by the two treatments (Fig. S6a). The pathway annotation of these MS features revealed that amino acid metabolism, carbon fixation, glucose metabolism, phenylpropanoid biosynthesis, and terpenoid backbone biosynthesis were significantly changed by *NaMYC2a/b* cosilencing (Fig. S6b). Targeted metabolite analyses verified these pathway inferences for sugars, amino acids, phenolamides, O-AS, and HGL-DTGs (Fig. S6c).

When MeJA-elicited plants were grown with competitors, the PCA analysis revealed that EV and irMYC2a/b metabolomes were separated along PC1 under both single and mixed-genotype combinations (Fig. 4b). Interestingly, when EV plants were grown with the EV genotypes (SEV), their MeJA-elicited metabolomes were slightly more divergent, than if they competed with irMYC2a/b plants (MEV); but the opposite pattern was observed for irMYC2a/b (Fig. 4b). In other words, under competitive-growth conditions, the metabolic response of irMYC2a/b plants competing with the same and different genotypes differed from that of EV plants.

Primary and specialized metabolites that respond to growth with different competitors

The metabolite levels of EV and irMYC2a/b in single- and mixed-genotype competitive growth were analyzed to provide a more granular view of the global patterns seen in the PCAs (Fig. 5a). The metabolite heatmap revealed that most carbohydrates, amino acids, O-AS, and phenolamides of plants grown in the competitive environment (Fig. 5b) have a pattern consistent with those from plants grown in a noncompetitive environment (Fig. S6c), namely increased primary metabolites but decreased specialized metabolites in irMYC2a/b. However, the responses of some HGL-DTGs, phenolamides, sugars, amino acids, and flavonoids in irMYC2a/b and EV showed strong differences when faced with different competitors (Fig. 5b). For example, in contrast to irMYC2a/b competing with itself (SirMYC2a/b), irMYC2a/b competing with EV (MirMYC2a/b) had leaves with significantly increased contents of tyrosine, tyramine, tryptophan,

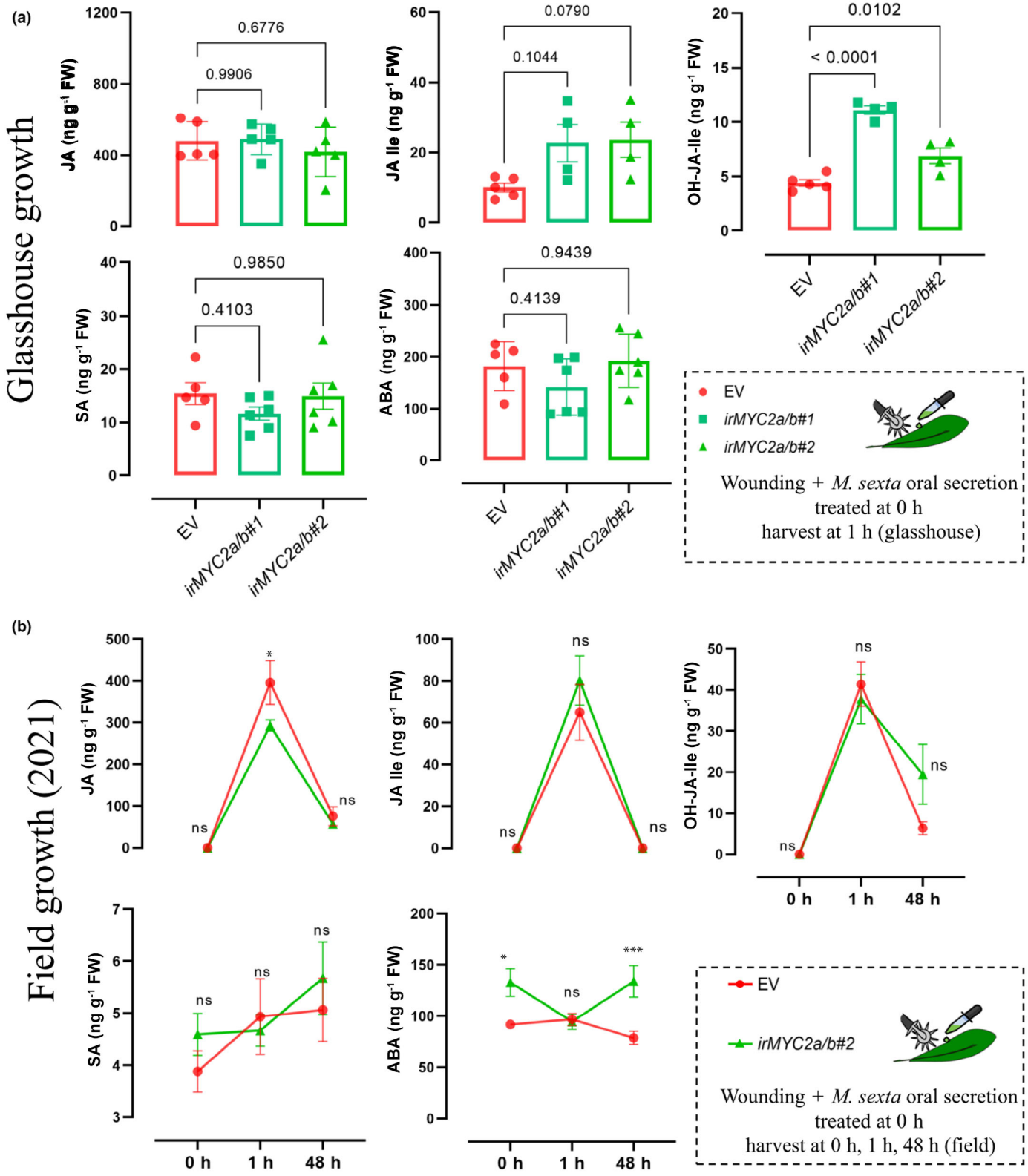

Fig. 2 Oral secretion (OS)-elicited leaf phytohormone concentrations in glasshouse- (a) and field-grown plants (b). (a) In glasshouse-grown plants ($n = 5$–6), OS-elicited leaves were harvested 1 h after the treatment. (b) In field-grown plants ($n = 10$) OS-elicited leaves were harvested at 0, 1, and 48 h. ABA, abscisic acid; JA, jasmonic acid; JA-Ile, jasmonoyl-isoleucine; OH-JA-Ile, hydroxy-jasmonoyl-isoleucine; SA, salicylic acid (mean ± SE, ANOVA Tukey's test: *, $P < 0.05$; ***, $P < 0.001$; ns, not significant).

New Phytologist

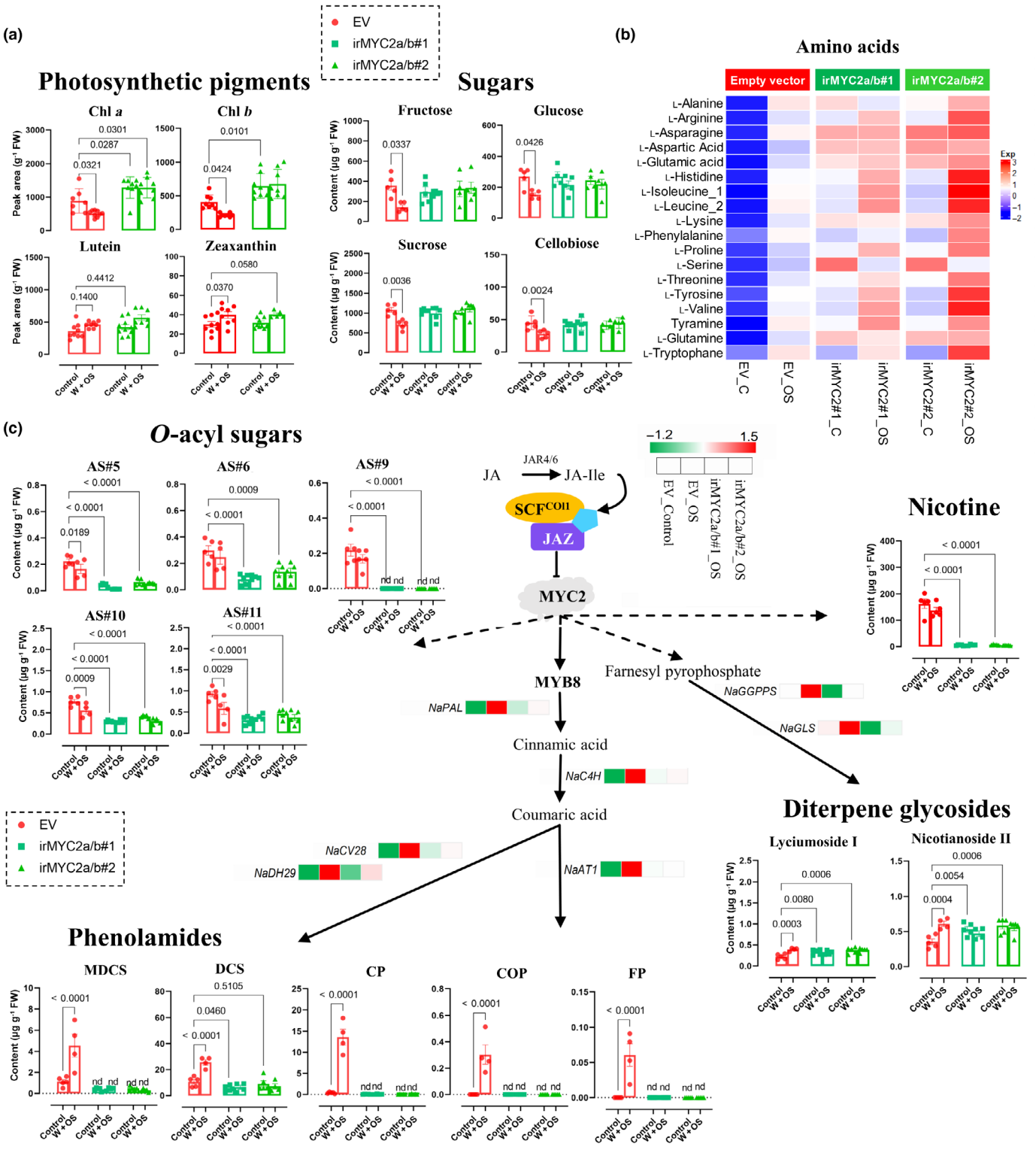

Fig. 3 Effects of wound (W) + oral secretion (OS) elicitation on primary (a, b) and specialized metabolites and selected transcripts (c). (a) Photosynthetic pigments and sugar contents, (b) amino acids, (c) overview pathway of quantified specialized metabolites. Genes (ID numbers given in the Materials and Methods section): *NaAT1*, agmatine coumaroyltransferase; *NaC4H*, *trans*-cinnamate 4-monooxygenase; *NaCV28*, acetyl-CoA-benzyl alcohol acetyltransferase-like; *NaDH29*, acetyl-CoA-benzyl alcohol acetyltransferase; *NaGGPPS*, geranylgeranyl diphosphate synthase; *NaGLS*, geranyl linalool synthase; *NaPAL*, phenylalanine ammonia-lyase; *NaPMT*, putrescine *N*-methyltransferase. Metabolites: COP, *N*-coumaroylputrescine; CP, *N*-caffeoylputrescine; DCS, *N*′,*N*″-di-caffeoylspermidine; FP, *N*-feruloylputrescine; MDCS, monohydrated *N*′,*N*″-di-caffeoylspermidine. Values are mean ± SE; $n = 5$ plants/treatment/genotype, two-way ANOVA, Tukey's test. nd, not detected; solid arrows, metabolic pathways with identified synthetic steps; dashed arrows, metabolic pathways with unidentified synthetic steps.

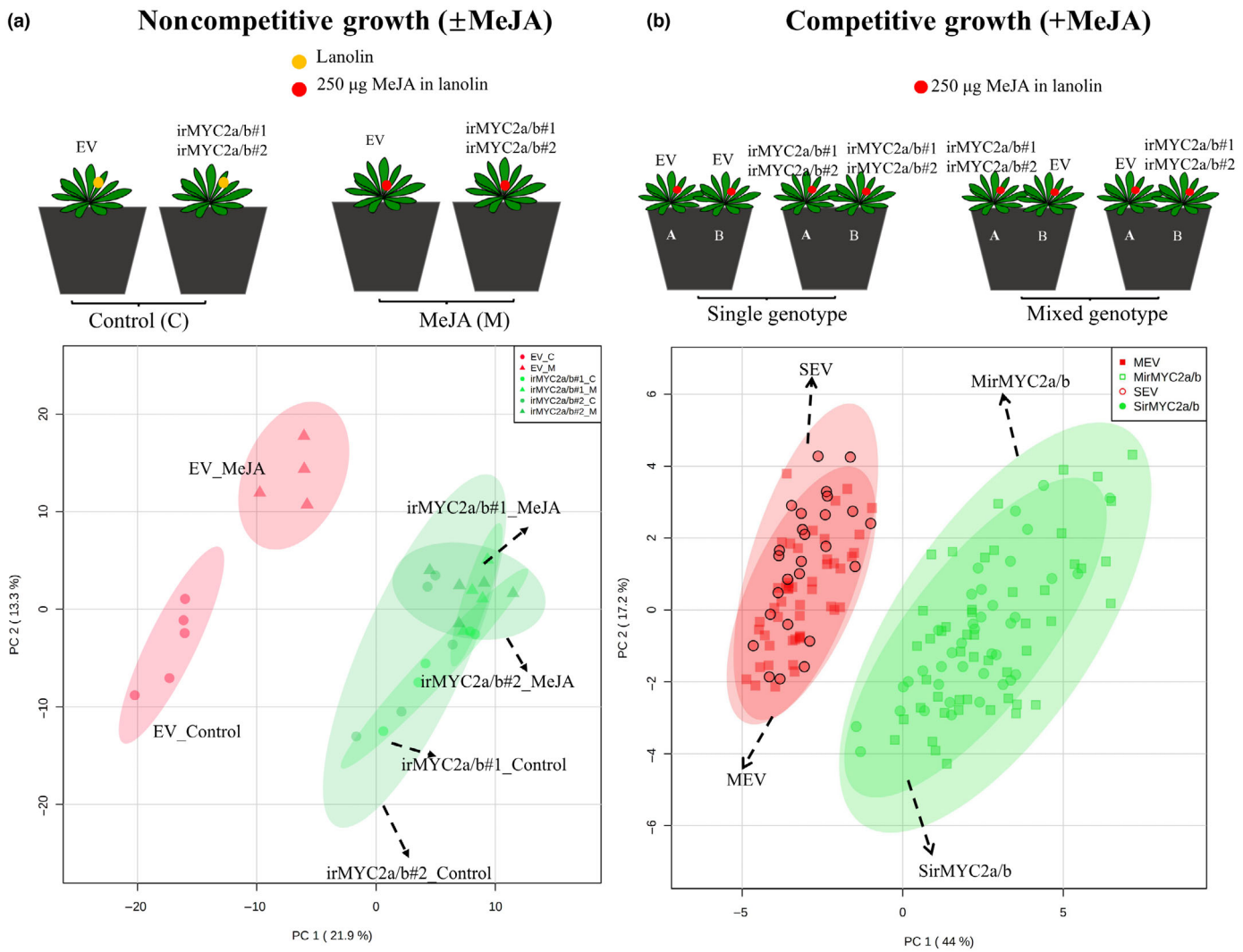

Fig. 4 Metabolite profiling in methyl jasmonate (MeJA)-elicited leaves of plants grown singly or with a size-matched competitor. (a) Principal component analysis (PCA) score plot of metabolites of plants in a noncompetitive-growth environment (Lanolin ± MeJA elicitation); (b) PCA score plot of metabolites of plants in a competitive-growth environment, the metabolite data comes from the same experiment as Figs 5 and 6. EV, empty vector; SEV, all EV plants in single-genotype pots (including plant A and plant B); MEV, all EV plants in mixed-genotype pots; SirMYC2a/b, all irMYC2a/b#1 and #2 plants in single-genotype pots; MirMYC2a/b, all irMYC2a/b#1 and #2 plants in mixed-genotype pots.

nicotianoside IX, nicotianoside X, *O*-coumaroylquinic acid, kaempferol-glucose-rhamnose, and rutin, and significantly decreased contents of glucose, glutathione, nicotianoside I, nicotianoside II, nicotianoside V, nicotianoside VII, nicotianoside XI, and di-feruloyl-spermidine (Fig. 5c). However, the same differences were not found in EV plants (Fig. 5b,c). Additionally, there was no significant difference in HGL-DTG and flavonoid contents between MeJA-induced EV and irMYC2a/b plants under noncompetitive (Fig. S6) and single-genotype competitive combinations (Fig. 5b). These results indicated that the identity of neighbor plants affects metabolic responses.

Growth and defense in a competitive environment with mobile larvae: neighbor identity matters

We next increased the ecological realism of our analysis of growth/defense trade-offs by adding a mobile herbivore (Fig. 6a) to the experimental setups. We first address the consequences for larval growth as an indicator of plant resistance. Regardless of the competition combination, larvae initially placed on irMYC2a/b plants were less likely to move to neighbor plants than those initially placed on EV plants (Fig. 6b). Fewer larvae transferred to neighbors compared with those placed on EV plants, and a greater number of larvae returned to the irMYC2a/b plants if the neighbor was an EV plant. Interestingly, this delayed movement was observed despite the fact that larvae grew faster on irMYC2a/b plants (which would allow them to move earlier). Larvae initially placed on irMYC2a/b plants generally did not move much until the third/fifth instars, while larvae initially placed on EV plants moved earlier, from first to second instars (Fig. 6b). Compared with larvae initially placed on EV plants, larvae initially placed on irMYC2a/b plants gained 1.5–4.6 times more mass (Fig. 6c). In mixed-genotypes combinations, the more larvae that moved from irMYC2a/b to EV plants at an early age, the lower the final larval

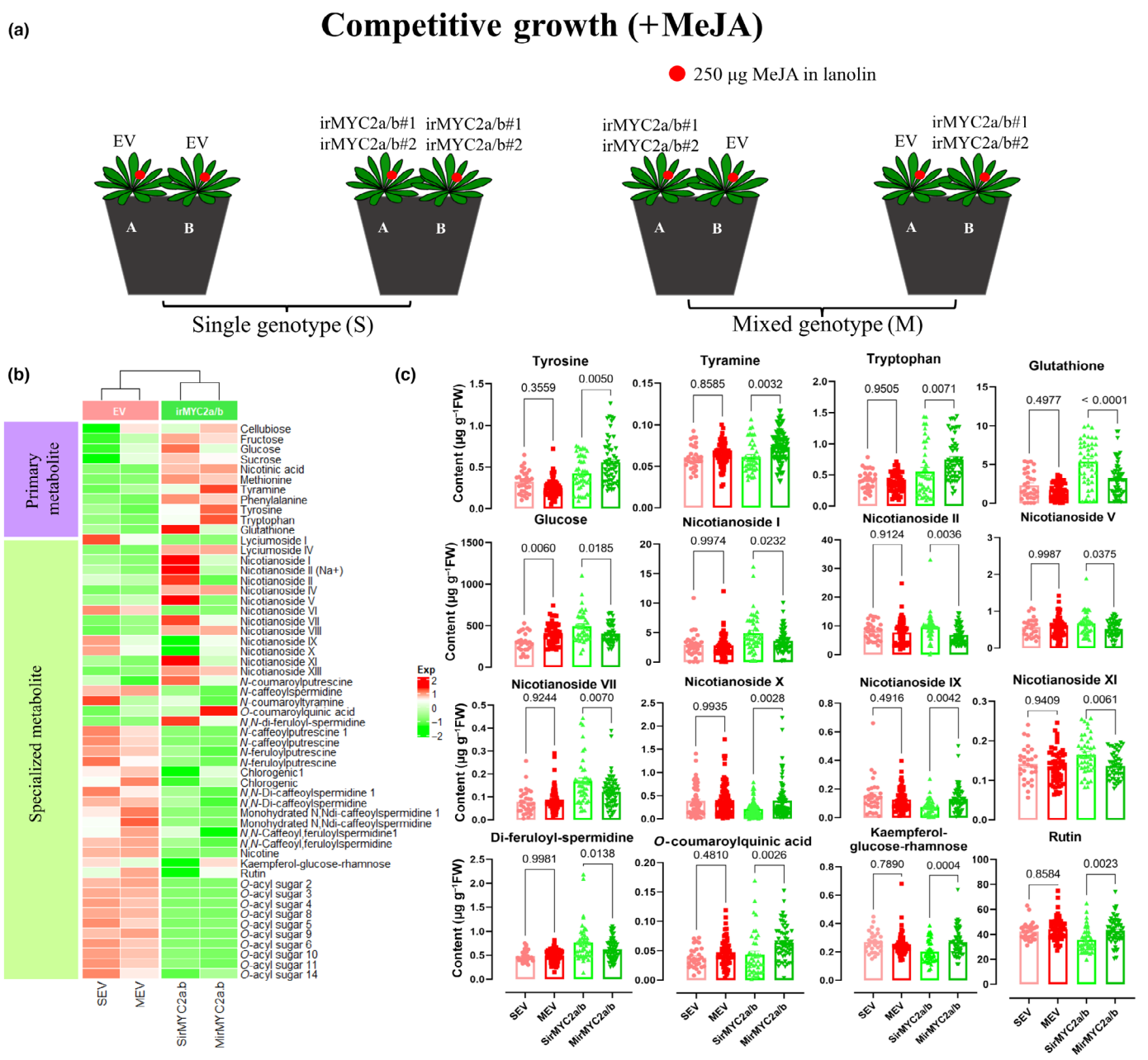

Fig. 5 Methyl jasmonate (MeJA)-elicited metabolites of leaves in single- and mixed-genotype competitive-growth combinations. (a) Schematic of the competitive-growth setup; (b) metabolite heatmap of EV and irMYC2a/b plants under different competitive-growth combinations. The data were normalized by log transformation (base 10) and Pareto scaling (mean-centered and divided by the square root of the standard deviation of each variable). (c) Metabolites with significant differences between single- and mixed-genotype pot (mean ± SE, $n = 30–60$, one-way ANOVA, Tukey's test). SEV, all empty vector (EV) plants in single-genotype pots (including Plant A and Plant B); MEV, all EV plants in mixed-genotype pots; SirMYC2a/b, all irMYC2a/b#1 and #2 plants in single-genotype pots; MirMYC2a/b, all irMYC2a/b#1 and #2 plants in mixed-genotype pots.

mass; conversely, the more larvae moved from EV plants to irMYC2a/b, the greater the final larval mass of this combination (Fig. 6b,c).

For plants, the identity of competing plants was crucial for growth and fitness. In the single-genotype combinations (EE, M1M1, and M2M2), irMYC2a/b plants compared with EV plants were 6.2% (M1M1) and 14.6% (M2M2) smaller in plant height, 9.1% (M1M1) and 24.2% (M2M2) lower in biomass, 21.3% (M1M1) and 36.2% (M2M2) lower in capsule number, and produced 13.1% (M1M1) and 21.3% (M2M2) fewer capsules per dry biomass. However, in the mixed-genotype combinations (EM1, EM2, M1E, and M2E), EV and irMYC2a/b did not differ (Fig. 6d). The total capsule and biomass production of plants growing in the competitive combinations of mixed-genotypes (EM1, EM2, M1E, and M2E) was significantly greater than those of the single-genotype combinations (EE, M1M1, and M2M2): in EV plants (average of EV in all mixed-genotypes combinations) increased by 4.6%, 7.0%, 18.7%, and 11.5% in

plant height, biomass, capsule number, and capsules per dry biomass, while in irMYC2a/b plants (average of irMYC2a/b in all mixed-genotypes combinations) increased by 20.6%, 27.7%, 67.8%, and 32.3%, respectively (Fig. 6d). The combined total-pot production values revealed that when planted in mixed-genotype combination, plants realized significantly greater fitness than when planted in single-genotype combinations in environments with a mobile herbivore (Fig. 6d).

We next analyzed plant fitness measures in the context of the resistance patterns created by the different treatment groups; recall that all plants were MeJA-elicited before larvae were 'oviposited' on a specific plant of each competitive combination. Larvae initially placed on EV plants were considered a 'priority defense' treatment (EM1, EM2), and those initially placed on irMYC2a/b plants, a 'delayed defense' treatment (M1E, M2E). Compared with those in priority defense treatments, plants in the delayed-defense treatment had 29.6% (EM1 vs M1E) and 6.6% (EM2 vs M2E) lower capsule numbers, and produced 24.7% (EM1 vs M1E) and 12.2% (EM2 vs M2E) fewer capsules per dry biomass (Fig. 6d). Moreover, the combination (EM2), in which early-instar larval movement occurred in the priority defense combination (EM1, EM2), had a 24.9% reduction in capsule number (33.4% in EV and 13.5% in irMYC2a/b plants) in EM2 compared with EM1, whose larvae moved less frequently to the neighboring plant. By contrast, in the delayed-defense combination (M1E, M2E), no differences in capsule numbers were observed in M2E which had more larvae moving to the neighboring plant than did M1E (Fig. 6d).

These results indicated that in environments with competitors and herbivores, a robust chemical defense is associated with fitness benefits. In competitive environments, plants of the high-defense combination (EE) had a fitness advantage over those of the weak-defense combinations (M1M1 and M2M2). Plants of the priority defense combinations (EM1 and EM2) realized a fitness advantage over those of the delayed-defense combinations (M1E, EM2). However, for plants with a weak-defense neighbor, it may be detrimental to motivate early larval movement to neighboring plants, as these can return at larger, more voracious stage.

Correlations among metabolites and plant growth and defense: not all specialized metabolites are defenses

To reveal the associations between particular metabolites and plant growth and defense from the previous experiment (Fig. 6), we correlated metabolite quantities with the measures of larval and plant performance. Specialized metabolites, such as O-AS, nicotine, flavonoids, most phenolamides, and a small sector of HGL-DTGs, were positively correlated with plant height, dry biomass, and capsules number, but negatively correlated with plant damage and larval mass and hence followed the pattern of the classical defense metabolite, nicotine (Fig. 7). Among these, nicotianoside IX, nicotianoside X, *O*-coumaroylquinic acid, kaempferol-glucose-rhamnose, and rutin were the metabolites found in irMYC2a/b that significantly increased in the competitive combination of mixed genotypes (Fig. 5). However, the quantities of di-feruloylspermidine, caffeoylspermidine, nicotianoside I, lyciumoside IV, nicotianoside VII, and nicotianoside VIII, on the contrary, exhibited patterns consistent with the classical primary metabolites, such as cellobiose, fructose, glucose, sucrose, methionine, and phenylalanine, which were negatively correlated with plant height, dry biomass, and capsule number, but positively correlated with plant damage and larvae mass (Fig. 7). Moreover, these metabolites were found to decrease in the competitive combinations of mixed genotypes. Coumaroylputrescine, coumaroyltyramine, nicotianoside II, and nicotianoside XI were negatively correlated with all phenotypic traits (Fig. 7) and were also found to decrease in the competitive combination of mixed genotypes (Fig. 5). These correlations suggest that biosynthetic pathways do not accurately predict metabolite functions.

Discussion

The evolutionary mechanisms responsible for plant growth/defense trade-offs have been the subject of a long and venerable body of theory (McKey, 1974, 1979; Rhoades & Cates, 1976; Herms & Mattson, 1992) which predates the molecular biology revolution (Schuman & Baldwin, 2016). Here, we explored the role of MYC2, a key regulator of JA signaling, to understand the metabolic underpinnings of growth/defense trade-offs in natural and experimental environments that captured some of the ecological complexity envisioned by early theoreticians as being central to the trade-offs, namely growth with competitors and mobile herbivores. By comparing an *N. attenuata*-specific HMM for the bHLH-MYC_N domain with the *N. attenuata* genome, we identified 25 MYC-like and three MYC2-like candidates of which two (*NaMYC2a* and *NaMYC2b*) were strongly induced by *M. sexta* OS elicitations (Fig. S3b). The effects of *NaMYC2a*/b cosilencing on growth, defense, and metabolic performance of plants in glasshouse and field environments confirmed MYC2's published effects on seedling development (Fig. 1a), shoot growth (Fig. 1b,c,g), defense (Fig. 1f,h), and metabolic regulation (Fig. 3) from other species, namely negative regulation of root and shoot growth (Dombrecht *et al.*, 2007; Gupta *et al.*, 2014; Srivastava *et al.*, 2019), JA-induced reductions in chlorophyll degradation and carbon assimilation (Zhu *et al.*, 2015; Zhuo *et al.*, 2020; Ding *et al.*, 2022) and herbivore resistance (Schweizer *et al.*, 2013; Sun *et al.*, 2020), and the synthesis of specialized metabolites responsible for resistance, such as nicotine (Shoji & Hashimoto, 2011), terpenoids (Hong *et al.*, 2012; Shen *et al.*, 2016; Sui *et al.*, 2018), phenylpropanoids (Wei *et al.*, 2022), and phenolamides (Woldemariam *et al.*, 2013). *O*-acyl sugars, a class of constitutively produced defense metabolites in *N. attenuata* (Weinhold & Baldwin, 2011; Luu *et al.*, 2017), were also abrogated in *NaMYC2a/b* cosilenced plants (Fig. 3d). MYC2 has been reported to regulate the biosynthesis of phytohormones, *via* feedback loops, particularly in wound-induced JA biosynthesis in *A. thaliana* (Dombrecht *et al.*, 2007; C. Zhang *et al.*, 2020); however, we found few consistent differences between EV and irMYC2a/b plants in their OS-elicited phytohormone levels (Fig. 2), consistent with previous research (Woldemariam *et al.*, 2013; Li *et al.*, 2017). These

New Phytologist

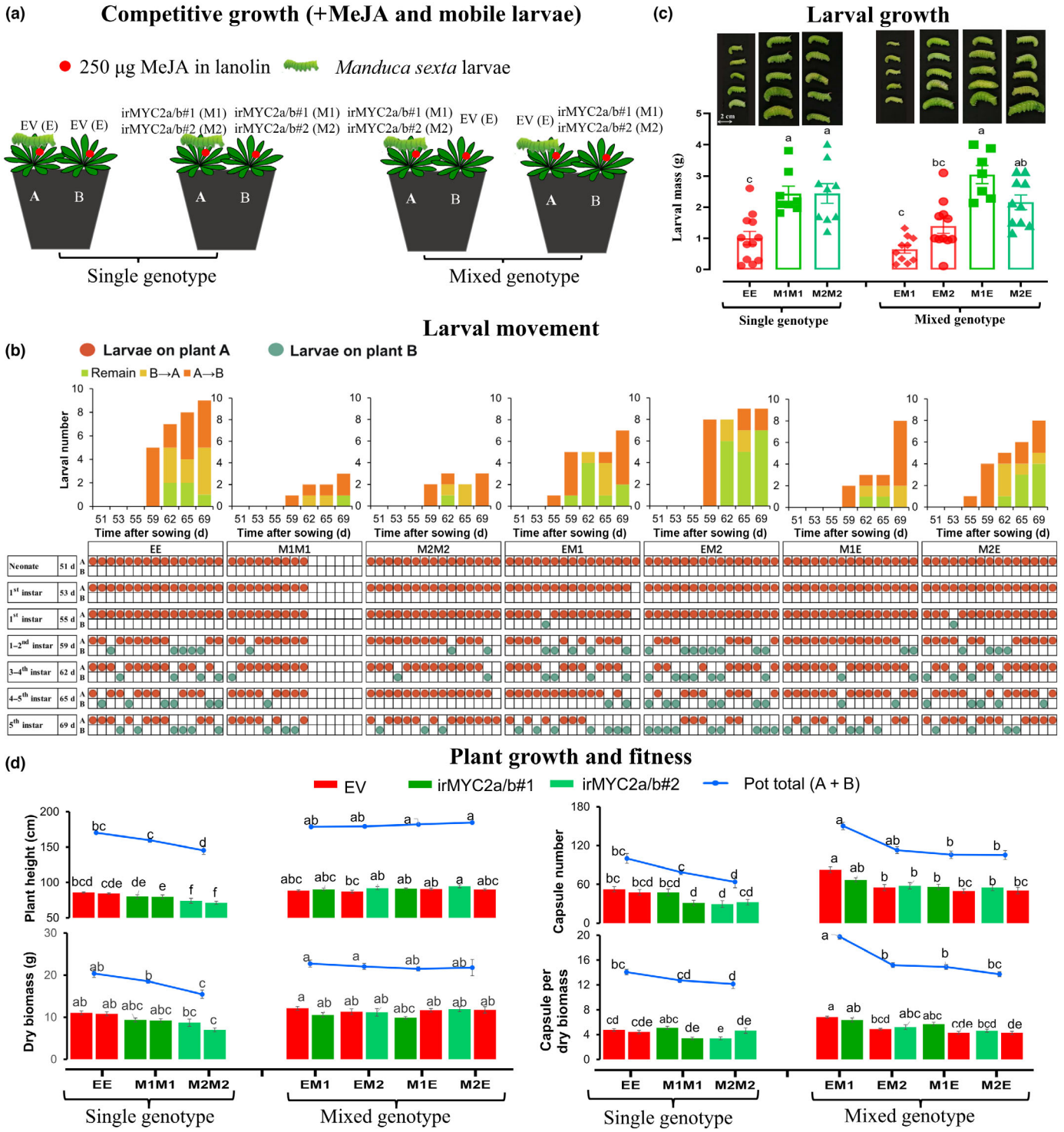

Fig. 6 Plant and larval growth, larval movement, and plant fitness measures of setups with competing, methyl jasmonate (MeJA)-elicited plants, and mobile larvae. (a) Schematic of the competitive experiment, irMYC2a/b, and empty vector (EV) seedlings were planted in 2 l pots in different combinations, two rosette leaves of each plant were treated with lanolin containing 250 µg MeJA for 72 h, after which a single neonate *Manduca sexta* larva was placed on one of the two size-matched genotypes growing in competition and allowed to feed and move freely between the two competing plants. (b) Instar-specific movement (pink: larvae remained on A plant; green: larvae moved to B plant) on EV and irMYC2a/b plants in the single- and mixed-genotype competition setups. Different lowercase letters indicate significant differences among levels of larval mass ($P < 0.05$). (c) Larval mass on EV and irMYC2a/b plants in the single- and mixed-genotype competition setups. (d) Plant growth (mass and height) and fitness (capsule number and biomass) of EV and irMYC2a/b plants in the single- and mixed-genotype competition setups and total plant growth and total fitness of each combination (mean ± SE, $n = 15$, two-way ANOVA, Tukey's test, different lowercase letters indicate significant differences among levels of fitness indices).

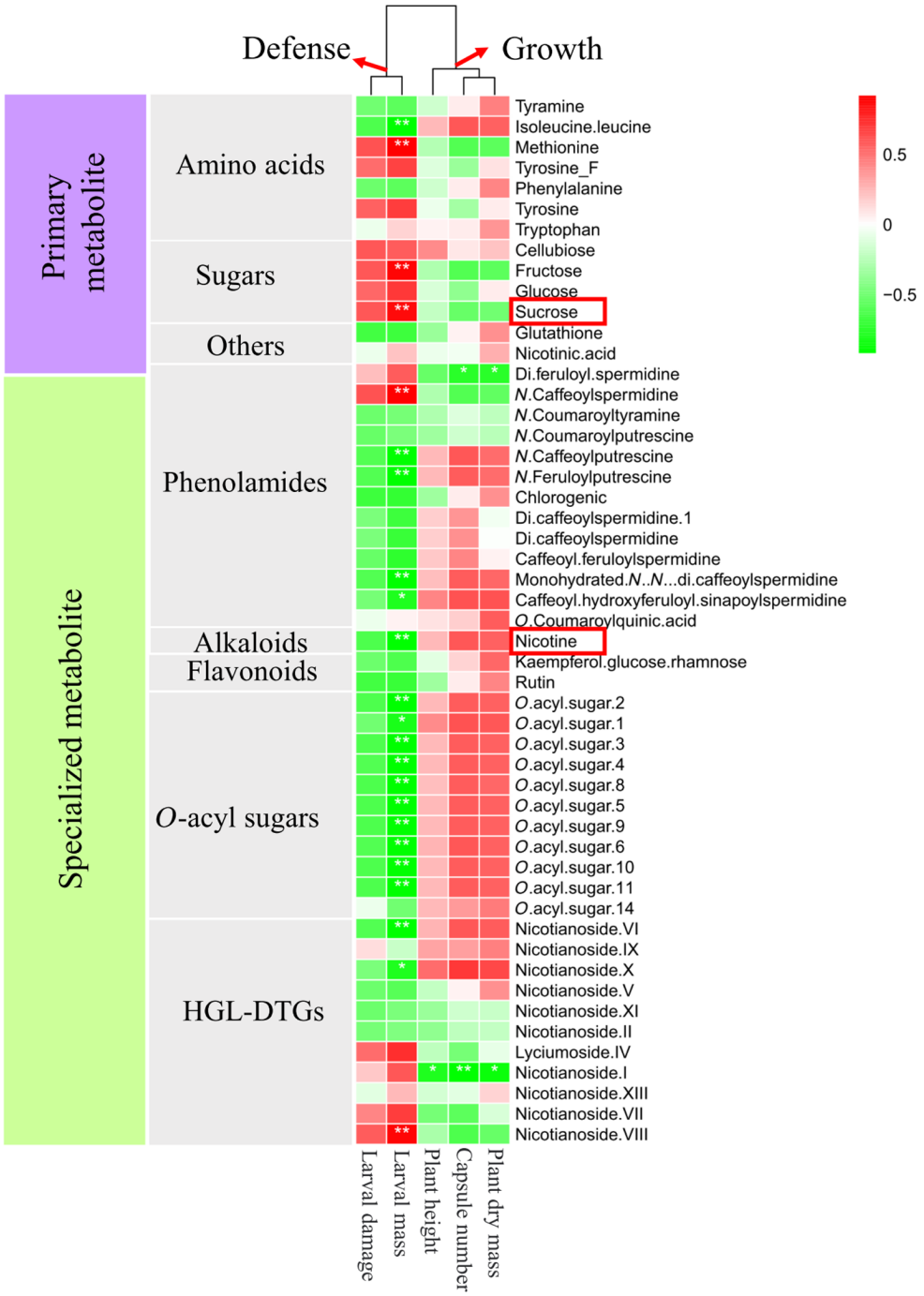

Fig. 7 Heatmap of correlations among methyl jasmonate (MeJA)-elicited metabolites with plant growth (height, capsule, and dry mass) and defense (larval damage and mass) phenotypes in competing and attacked *Nicotiana attenuata* plants. The phenotypes and metabolite data were from the competitive-growth experiment described in Fig. 6; leaf metabolite data were collected 72 h after MeJA treatment and before plants were infested with *Manduca sexta* larvae. The red boxes highlight regression relationships of a classical primary (sucrose) and a specialized metabolite (nicotine) functioning in plant growth and defense, respectively. The color gradient from red to green indicates metabolite concentrations from high to low.

results suggest that *NaMYC2a/b* in *N. attenuata* may consolidate the functions of several MYC2 TFs reported in other species and have minimal effects on phytohormone levels, a distinct advantage when exploring the JA-mediated growth/defense trade-offs in ecologically complex environments.

When irMYC2a/b plants were grown in single pots without competitors or herbivores in the glasshouse, their realized fitness, estimated by seed production, was not significantly greater than that of the slower-growing EV plants (Fig. 1e); however, their growth and likely fitness advantage became dramatically apparent when planted in the field during a year of very low-herbivore loads (Fig. 1g,h), confirming previous studies of costly defenses (Baldwin, 1998; Zavala & Baldwin, 2004). Here, we show that isogenic competitors differing only in *NaMYC2a/b* expression

and all of the above-mentioned metabolic responses, elicited different metabolic responses in competing neighbors (Figs 4b, 5b, c). In contrast to the overall metabolic stability of EV plants, irMYC2a/b plants produced metabolic responses significantly different when competing with themselves and EV plants. The responses in flavonoids, HGL-DTGs, and phenolamide accumulation of irMYC2a/b plants were particularly noteworthy (Fig. 5b,c). These 'neighbor-responses' were associated with significant fitness outcomes, as the combined growth and capsule production of competing EV and irMYC2a/b plants were greater than those of the single-genotype combinations, composed of irMYC2a/b or EV plants (Fig. 6d). While the fitness of individual irMYC2a/b or EV plants depended very much on the feeding and movement behavior of the mobile herbivore; overall, there were only minor fitness differences between irMYC2a/b and EV plants in the mixed-genotype competition combinations (Fig. 6d). This underscores the important point that while resistance traits may incur large fitness costs that result from the allocation of fitness-limiting resources or autotoxicity, in complex ecological environments, third-party effects frequently compensate for these costs, resulting in no detectable differences in fitness (Züst & Agrawal, 2017; Figs 4–6). These third-party effects clearly include herbivore defense effects (Baldwin, 1998), but others, such as signal-sharing benefits (Pierik *et al.*, 2013), the effectiveness of nutrient acquisition (D. Zhang *et al.*, 2020), and root exudates and microbiome effects (Broz *et al.*, 2010; Huang & Osbourn, 2019), deserve additional research.

The results of our metabolite correlation analysis (Fig. 7) showed that the HGL-DTGs or phenolamides, which accumulated differently in plants depending on their single- or mixed-genotype environment, were functioning more like nutritional or signaling substances, rather than defense metabolites. These functional associations of metabolites that differ from the functions that might be inferred from biosynthetic pathways are fully commensurate with Matthias Erb and Daniel Kliebenstein's insightful perspective on plant metabolism, namely that of a 'blurred functional trichotomy' (Erb & Kliebenstein, 2020). A growing body of evidence has revealed that many specialized metabolites have multiple functions beyond their functions in defense (Peer & Murphy, 2007; Kemen *et al.*, 2014; Maag *et al.*, 2015; Li *et al.*, 2018; Muhlemann *et al.*, 2018), for example, as primary metabolites (Soubeyrand *et al.*, 2018), regulators of growth and development (Li *et al.*, 2018; Muhlemann *et al.*, 2018), and promoters of trace element uptake (Mladěnka *et al.*, 2010; Hu *et al.*, 2018), or as chemical signals that attract beneficial insects and microorganisms (Baldwin *et al.*, 2006; Eckardt, 2006; Moses *et al.*, 2014). The role of HGL-DTG glycosides (Li *et al.*, 2018) and flavonoids (Yin *et al.*, 2014; Park *et al.*, 2020) in the regulation of flower development or growth in plants has been well-established. The differential accumulation of flavonoids, phenolamides, and HGL-DTGs in plants grown in mixed-genotype combinations may contribute *via* some of these nondefense functions to the fitness advantages of growth in mixed-genotype combinations.

The synthesis of metabolites that function as defenses can command a substantial fraction of a plant's carbon or nitrogen budget (Gershenzon, 1994; Baldwin *et al.*, 1998; Ullmann-Zeunert *et al.*, 2012); however, this resource investment rarely leads to observable fitness costs or the expected allocation patterns when plants face resource constraints. For example, reductions in environmental N availability do not reduce, but rather increase a plant's allocation to N-intensive defensive compounds, such as nicotine (Baldwin & Ohnmeiss, 1994b; Ohnmeiss & Baldwin, 1994; Baldwin *et al.*, 1998). Here, we see that irMYC2a/b plants grow faster than their specialized-metabolite-producing EV plants (Figs 1, 6d); however, despite their attenuated metabolic potential, irMYC2a/b plants adjust their metabolite accumulations depending on the growth/defense status of their neighbors, much as other studies have suggested (Broz *et al.*, 2010).

Given that plants can adjust their metabolism in sophisticated ways in response to their environmental context, it is worth considering how best to incorporate this environmental responsiveness into future research efforts on the growth/defense trade-off. In complex ecological environments, third-party trade-offs are the norm. Traits that provide resistance against some herbivores may increase susceptibility to other types of herbivores, pathogens, and abiotic stresses (Thaler *et al.*, 2002; Frost *et al.*, 2008), or influence important mutualists, such as pollinators, natural enemies (Strauss *et al.*, 1999; Gols, 2014), and symbiotic microorganisms, such as arbuscular mycorrhizal fungi (Bais *et al.*, 2008; Tian *et al.*, 2021). These third-party players are usually excluded from laboratory studies and conducting trade-offs studies under field conditions is perhaps the most robust means of not excluding players that have been important in the evolution of the environmental signaling systems that plants use to navigate these growth/defense trade-offs. In this context, we note that the most visually apparent differences in growth/defense phenotypes between irMYC2a/b and EV plants occurred during the two field seasons (Fig. 1g,h) when size-match seedlings were planted in their native habitat.

Acknowledgements

We acknowledge the China Scholarship Council (no. 201906910083) and the International Max Planck Research School (IMPRS) for financial support, Wibke Seibt for support in transgenic plant screening, and Prof. Dr Sarah O'Connor for comments on a draft of the manuscript. Open Access funding enabled and organized by Projekt DEAL.

Competing interests

None declared.

Author contributions

CY and ITB designed glasshouse experiments and wrote paper. YB and ITB designed field experiments. CY conducted all glasshouse experiments and analyzed all data, while ITB and GB conducted all field experiments. YB focused the project on MYC2a/b and provided training to CY in experimental design. YB, RH,

and KG provided valuable technical support in transgenic lines construction, line screening, and metabolite analysis. All authors provided comments on the manuscript.

ORCID

Yuechen Bai https://orcid.org/0000-0002-2314-8660
Gundega Baldwin https://orcid.org/0000-0002-0704-2508
Ian T. Baldwin https://orcid.org/0000-0001-5371-2974
Klaus Gase https://orcid.org/0000-0002-8028-5645
Rayko Halitschke https://orcid.org/0000-0002-1109-8782
Caiqiong Yang https://orcid.org/0000-0003-3847-4167

Data availability

The data that support the findings of this study are available in Figshare at doi: 10.6084/m9.figshare.21829692.

References

Attaran E, Major IT, Cruz JA, Rosa BA, Koo AJ, Chen J, Kramer DM, He SY, Howe GA. 2014. Temporal dynamics of growth and photosynthesis suppression in response to jasmonate signaling. *Plant Physiology* **165**: 1302–1314.

Backmann P, Grimm V, Jetschke G, Lin Y, Vos M, Baldwin IT, van Dam NM. 2019. Delayed chemical defense: timely expulsion of herbivores can reduce competition with neighboring plants. *The American Naturalist* **193**: 125–139.

Bai Y, Yang C, Halitschke R, Paetz C, Kessler D, Burkard K, Gaquerel E, Baldwin IT, Li D. 2022. Natural history-guided omics reveals plant defensive chemistry against leafhopper pests. *Science* **375**: eabm2948.

Bais HP, Broeckling CD, Vivanco JM. 2008. Root exudates modulate plant–microbe interactions in the rhizosphere. In: Karlovsky P, ed. *Secondary metabolites in soil ecology*. Berlin & Heidelberg, Germany: Springer, 241–252.

Baldwin IT. 1996. Methyl jasmonate-induced nicotine production in *Nicotiana attenuata*: inducing defenses in the field without wounding. *Entomologia Experimentalis et Applicata* **80**: 213–220.

Baldwin IT. 1998. Jasmonate-induced responses are costly but benefit plants under attack in native populations. *Proceedings of the National Academy of Sciences, USA* **95**: 8113–8118.

Baldwin IT, Callahan P. 1993. Autotoxicity and chemical defense: nicotine accumulation and carbon gain in solanaceous plants. *Oecologia* **94**: 534–541.

Baldwin IT, Gorham D, Schmelz EA, Lewandowski CA, Lynds GY. 1998. Allocation of nitrogen to an inducible defense and seed production in *Nicotiana attenuata*. *Oecologia* **115**: 541–552.

Baldwin IT, Halitschke R, Paschold A, von Dahl CC, Preston CA. 2006. Volatile signaling in plant–plant interactions: "talking trees" in the genomics era. *Science* **311**: 812–815.

Baldwin IT, Hamilton W. 2000. Jasmonate-induced responses of *Nicotiana sylvestris* results in fitness costs due to impaired competitive ability for nitrogen. *Journal of Chemical Ecology* **26**: 915–952.

Baldwin IT, Ohnmeiss TE. 1994a. Coordination of photosynthetic and alkaloidal responses to damage in uninducible and inducible *Nicotiana Sylvestris*. *Ecology* **75**: 1003–1014.

Baldwin IT, Ohnmeiss TE. 1994b. Swords into plowshares? *Nicotiana sylvestris* does not use nicotine as a nitrogen source under nitrogen-limited growth. *Oecologia* **98**: 385–392.

Baldwin IT, Zhang Z-P, Diab N, Ohnmeiss TE, McCloud ES, Lynds GY, Schmelz EA. 1997. Quantification, correlations and manipulations of wound-induced changes in jasmonic acid and nicotine in *Nicotiana sylvestris*. *Planta* **201**: 397–404.

Bekaert M, Edger PP, Hudson CM, Pires JC, Conant GC. 2012. Metabolic and evolutionary costs of herbivory defense: systems biology of glucosinolate synthesis. *New Phytologist* **196**: 596–605.

Bömer M, O'Brien JA, Pérez-Salamó I, Krasauskas J, Finch P, Briones A, Daudi A, Souda P, Tsui T-L, Whitelegge JP. 2018. COI1-dependent jasmonate signalling affects growth, metabolite production and cell wall protein composition in Arabidopsis. *Annals of Botany* **122**: 1117–1129.

Broz AK, Broeckling CD, De-la-Peña C, Lewis MR, Greene E, Callaway RM, Sumner LW, Vivanco JM. 2010. Plant neighbor identity influences plant biochemistry and physiology related to defense. *BMC Plant Biology* **10**: 115.

Bubner B, Gase K, Baldwin IT. 2004. Two-fold differences are the detection limit for determining transgene copy numbers in plants by real-time PCR. *BMC Biotechnology* **4**: 14.

Campos ML, Yoshida Y, Major IT, de Oliveira Ferreira D, Weraduwage SM, Froehlich JE, Johnson BF, Kramer DM, Jander G, Sharkey TD *et al.* 2016. Rewiring of jasmonate and phytochrome B signalling uncouples plant growth-defense tradeoffs. *Nature Communications* **7**: 12570.

Cao J, Li M, Chen J, Liu P, Li Z. 2016. Effects of MeJA on *Arabidopsis* metabolome under endogenous JA deficiency. *Scientific Reports* **6**: 37674.

Chen C, Chen H, Zhang Y, Thomas HR, Frank MH, He Y, Xia R. 2020. TBtools: an integrative toolkit developed for interactive analyses of big biological data. *Molecular Plant* **13**: 1194–1202.

Chen Q, Sun J, Zhai Q, Zhou W, Qi L, Xu L, Wang B, Chen R, Jiang H, Qi J *et al.* 2011. The basic helix-loop-helix transcription factor MYC2 directly represses *PLETHORA* expression during jasmonate-mediated modulation of the root stem cell niche in *Arabidopsis*. *Plant Cell* **23**: 3335–3352.

Cipollini D, Walters D, Voelckel C. 2017. Costs of resistance in plants: from theory to evidence. *Annual Plant Reviews Online* **47**: 263–307.

Clay NK, Adio AM, Denoux C, Jander G, Ausubel FM. 2009. Glucosinolate metabolites required for an *Arabidopsis* innate immune response. *Science* **323**: 95–101.

van Dam NM, Hadwich K, Baldwin IT. 2000. Induced responses in *Nicotiana attenuata* affect behavior and growth of the specialist herbivore *Manduca sexta*. *Oecologia* **122**: 371–379.

Ding F, Wang C, Xu N, Zhang S, Wang M. 2022. SlMYC2 mediates jasmonate-induced tomato leaf senescence by promoting chlorophyll degradation and repressing carbon fixation. *Plant Physiology and Biochemistry* **180**: 27–34.

Dombrecht B, Xue GP, Sprague SJ, Kirkegaard JA, Ross JJ, Reid JB, Fitt GP, Sewelam N, Schenk PM, Manners JM *et al.* 2007. MYC2 differentially modulates diverse jasmonate-dependent functions in Arabidopsis. *Plant Cell* **19**: 2225–2245.

Du M, Zhao J, Tzeng DTW, Liu Y, Deng L, Yang T, Zhai Q, Wu F, Huang Z, Zhou M *et al.* 2017. MYC2 orchestrates a hierarchical transcriptional cascade that regulates jasmonate-mediated plant immunity in tomato. *Plant Cell* **29**: 1883–1906.

Eckardt NA. 2006. The role of flavonoids in root nodule development and auxin transport in *Medicago truncatula*. *Plant Cell* **18**: 1539–1540.

Erb M, Kliebenstein DJ. 2020. Plant secondary metabolites as defenses, regulators, and primary metabolites: the blurred functional trichotomy. *Plant Physiology* **184**: 39–52.

File AL, Murphy GP, Dudley SA. 2012. Fitness consequences of plants growing with siblings: reconciling kin selection, niche partitioning and competitive ability. *Proceedings of the Royal Society B: Biological Sciences* **279**: 209–218.

Frost CJ, Mescher MC, Carlson JE, De Moraes CM. 2008. Plant defense priming against herbivores: getting ready for a different battle. *Plant Physiology* **146**: 818–824.

Gaquerel E, Gulati J, Baldwin IT. 2014. Revealing insect herbivory-induced phenolamide metabolism: from single genes to metabolic network plasticity analysis. *The Plant Journal* **79**: 679–692.

Gaquerel E, Heiling S, Schoettner M, Zurek G, Baldwin IT. 2010. Development and validation of a liquid chromatography–electrospray ionization–time-of-flight mass spectrometry method for induced changes in *Nicotiana attenuata* leaves during simulated herbivory. *Journal of Agricultural and Food Chemistry* **58**: 9418–9427.

Gershenzon J. 1994. The cost of plant chemical defense against herbivory: a biochemeical perspective. In: Bernays EA, ed. *Insect–plant interactions*. Boca Raton, FL, USA: CRC Press, 105–173.

Gog L, Berenbaum MR, DeLucia EH, Zangerl AR. 2005. Autotoxic effects of essential oils on photosynthesis in parsley, parsnip, and rough lemon. *Chemoecology* **15**: 115–119.

Golovatskaya IF, Karnachuk RA. 2008. Effect of jasmonic acid on morphogenesis and photosynthetic pigment level in Arabidopsis seedlings grown under green light. *Russian Journal of Plant Physiology* **55**: 220–224.

Gols R. 2014. Direct and indirect chemical defences against insects in a multitrophic framework. *Plant, Cell & Environment* **37**: 1741–1752.

Gupta N, Prasad VBR, Chattopadhyay S. 2014. LeMYC2 acts as a negative regulator of blue light mediated photomorphogenic growth, and promotes the growth of adult tomato plants. *BMC Plant Biology* **14**: 38.

Halitschke R, Baldwin IT. 2003. Antisense LOX expression increases herbivore performance by decreasing defense responses and inhibiting growth-related transcriptional reorganization in *Nicotiana attenuata*. *The Plant Journal* **36**: 794–807.

Halitschke R, Baldwin IT. 2004. Jasmonates and related compounds in plant–insect interactions. *Journal of Plant Growth Regulation* **23**: 238–245.

Halitschke R, Schittko U, Pohnert G, Boland W, Baldwin IT. 2001. Molecular interactions between the specialist herbivore *Manduca sexta* (Lepidoptera, Sphingidae) and its natural host *Nicotiana attenuata*. III. Fatty acid-amino acid conjugates in herbivore oral secretions are necessary and sufficient for herbivore-specific plant responses. *Plant Physiology* **125**: 711–717.

Hayashi S, Watanabe M, Kobayashi M, Tohge T, Hashimoto T, Shoji T. 2020. Genetic manipulation of transcriptional regulators alters nicotine biosynthesis in tobacco. *Plant and Cell Physiology* **61**: 1041–1053.

Heil M, Baldwin IT. 2002. Fitness costs of induced resistance: emerging experimental support for a slippery concept. *Trends in Plant Science* **7**: 61–67.

Heiling S, Llorca LC, Li J, Gase K, Schmidt A, Schäfer M, Schneider B, Halitschke R, Gaquerel E, Baldwin IT. 2021. Specific decorations of 17-hydroxygeranyllinalool diterpene glycosides solve the autotoxicity problem of chemical defense in *Nicotiana attenuata*. *Plant Cell* **33**: 1748–1770.

Heiling S, Schuman MC, Schoettner M, Mukerjee P, Berger B, Schneider B, Jassbi AR, Baldwin IT. 2010. Jasmonate and ppHsystemin regulate key malonylation steps in the biosynthesis of 17-hydroxygeranyllinalool diterpene glycosides, an abundant and effective direct defense against herbivores in *Nicotiana attenuata*. *Plant Cell* **22**: 273–292.

Herms DA, Mattson WJ. 1992. The dilemma of plants: to grow or defend. *The Quarterly Review of Biology* **67**: 283–335.

Hong GJ, Xue XY, Mao YB, Wang LJ, Chen XY. 2012. *Arabidopsis* MYC2 interacts with DELLA proteins in regulating sesquiterpene synthase gene expression. *Plant Cell* **24**: 2635–2648.

Hu L, Mateo P, Ye M, Zhang X, Berset JD, Handrick V, Radisch D, Grabe V, Köllner TG, Gershenzon J *et al.* 2018. Plant iron acquisition strategy exploited by an insect herbivore. *Science* **361**: 694–697.

Huang ACC, Osbourn A. 2019. Plant terpenes that mediate below-ground interactions: prospects for bioengineering terpenoids for plant protection. *Pest Management Science* **75**: 2368–2377.

Huang H, Liu B, Liu L, Song S. 2017. Jasmonate action in plant growth and development. *Journal of Experimental Botany* **68**: 1349–1359.

Huo YB, Zhang J, Zhang B, Chen L, Zhang X, Zhu CAS. 2021. MYC2 transcription factors TwMYC2a and TwMYC2b negatively regulate triptolide biosynthesis in *Tripterygium wilfordii* hairy roots. *Plants* **10**: 679.

Huot B, Yao J, Montgomery BL, He SY. 2014. Growth-defense tradeoffs in plants: a balancing act to optimize fitness. *Molecular Plant* **7**: 1267–1287.

Kallenbach M, Bonaventure G, Gilardoni PA, Wissgott A, Baldwin IT. 2012. *Empoasca* leafhoppers attack wild tobacco plants in a jasmonate-dependent manner and identify jasmonate mutants in natural populations. *Proceedings of the National Academy of Sciences, USA* **109**: E1548–E1557.

Kang J-H, Wang L, Giri A, Baldwin IT. 2006. Silencing threonine deaminase and JAR4 in *Nicotiana attenuata* impairs jasmonic acid-isoleucine-mediated defenses against *Manduca sexta*. *Plant Cell* **18**: 3303–3320.

Kaur H, Heinzel N, Schöttner M, Baldwin IT, Gális I. 2010. R2R3-NaMYB8 regulates the accumulation of phenylpropanoid-polyamine conjugates, which are essential for local and systemic defense against insect herbivores in *Nicotiana attenuata*. *Plant Physiology* **152**: 1731–1747.

Kazan K, Manners JM. 2013. MYC2: the master in action. *Molecular Plant* **6**: 686–703.

Kemen AC, Honkanen S, Melton RE, Findlay KC, Mugford ST, Hayashi K, Haralampidis K, Rosser SJ, Osbourn A. 2014. Investigation of triterpene synthesis and regulation in oats reveals a role for β-amyrin in determining root epidermal cell patterning. *Proceedings of the National Academy of Sciences, USA* **111**: 8679–8684.

Kessler A, Halitschke R, Baldwin IT. 2004. Silencing the jasmonate cascade: induced plant defenses and insect populations. *Science* **305**: 665–668.

Krügel T, Lim M, Gase K, Halitschke R, Baldwin IT. 2002. *Agrobacterium*-mediated transformation of *Nicotiana attenuata*, a model ecological expression system. *Chemoecology* **12**: 177–183.

Kumar P, Rathi P, Schöttner M, Baldwin IT, Pandit S. 2014. Differences in nicotine metabolism of two *Nicotiana attenuata* herbivores render them differentially susceptible to a common native predator. *PLoS ONE* **9**: e95982.

Li J, Halitschke R, Li D, Paetz C, Su H, Heiling S, Xu S, Baldwin IT. 2021. Controlled hydroxylations of diterpenoids allow for plant chemical defense without autotoxicity. *Science* **371**: 255–260.

Li J, Schuman MC, Halitschke R, Li X, Guo H, Grabe V, Hammer A, Baldwin IT. 2018. The decoration of specialized metabolites influences stylar development. *eLife* **7**: e38611.

Li R, Wang M, Wang Y, Schuman MC, Weinhold A, Schäfer M, Jiménez-Alemán GH, Barthel A, Baldwin IT. 2017. Flower-specific jasmonate signaling regulates constitutive floral defenses in wild tobacco. *Proceedings of the National Academy of Sciences, USA* **114**: E7205–E7214.

Li S, Wang P, Yuan W. 2010. Induced endogenous autotoxicity in *Camptotheca*. *Frontiers in Bioscience* **2**: 1196–1210.

Li X, Schuler MA, Berenbaum MR. 2002. Jasmonate and salicylate induce expression of herbivore cytochrome P450 genes. *Nature* **419**: 712–715.

Lou Y, Baldwin IT. 2003. *Manduca sexta* recognition and resistance among allopolyploid *Nicotiana* host plants. *Proceedings of the National Academy of Sciences, USA* **100**(Suppl 2): 14581–14586.

Luu VT, Weinhold A, Ullah C, Dressel S, Schoettner M, Gase K, Gaquerel E, Xu S, Baldwin IT. 2017. O-acyl sugars protect a wild tobacco from both native fungal pathogens and a specialist herbivore. *Plant Physiology* **174**: 370–386.

Maag D, Erb M, Köllner TG, Gershenzon J. 2015. Defensive weapons and defense signals in plants: some metabolites serve both roles. *BioEssays* **37**: 167–174.

Machado RA, Baldwin IT, Erb M. 2017. Herbivory-induced jasmonates constrain plant sugar accumulation and growth by antagonizing gibberellin signaling and not by promoting secondary metabolite production. *New Phytologist* **215**: 803–812.

McCloud ES, Baldwin IT. 1997. Herbivory and caterpillar regurgitants amplify the wound-induced increases in jasmonic acid but not nicotine in *Nicotiana sylvestris*. *Planta* **203**: 430–435.

McKey D. 1974. Adaptive patterns in alkaloid physiology. *The American Naturalist* **108**: 305–320.

McKey D. 1979. The distribution of secondary compounds within plants. In: Rosenthal GA, Janzen DH, eds. *Herbivores: their interaction with secondary plant metabolites*. New York, NY, USA: Academic Press, 55–134.

Mistry J, Chuguransky S, Williams L, Qureshi M, Salazar Gustavo A, Sonnhammer ELL, Tosatto SCE, Paladin L, Raj S, Richardson LJ *et al.* 2020. Pfam: the protein families database in 2021. *Nucleic Acids Research* **49**: D412–D419.

Mladěnka P, Macáková K, Zatloukalová L, Řeháková Z, Singh BK, Prasad AK, Parmar VS, Jahodář L, Hrdina R, Saso L. 2010. *In vitro* interactions of coumarins with iron. *Biochimie* **92**: 1108–1114.

Moses T, Papadopoulou KK, Osbourn A. 2014. Metabolic and functional diversity of saponins, biosynthetic intermediates and semi-synthetic derivatives. *Critical Reviews in Biochemistry and Molecular Biology* **49**: 439–462.

Muhlemann JK, Younts TLB, Muday GK. 2018. Flavonols control pollen tube growth and integrity by regulating ROS homeostasis during high-temperature stress. *Proceedings of the National Academy of Sciences, USA* **115**: E11188–E11197.

Nerva L, Giudice G, Quiroga G, Belfiore N, Lovat L, Perria R, Volpe MG, Moffa L, Sandrini M, Gaiotti F *et al.* 2022. Mycorrhizal symbiosis balances

rootstock-mediated growth-defence tradeoffs. *Biology and Fertility of Soils* **58**: 17–34.

Noir S, Bömer M, Takahashi N, Ishida T, Tsui T-L, Balbi V, Shanahan H, Sugimoto K, Devoto A. 2013. Jasmonate controls leaf growth by repressing cell proliferation and the onset of endoreduplication while maintaining a potential stand-by mode. *Plant Physiology* **161**: 1930–1951.

Oblessuc PR, Obulareddy N, DeMott L, Matiolli CC, Thompson BK, Melotto M. 2020. JAZ4 is involved in plant defense, growth, and development in Arabidopsis. *The Plant Journal* **101**: 371–383.

Ohnmeiss TE, Baldwin IT. 1994. The allometry of nitrogen to growth and an inducible defense under nitrogen-limited growth. *Ecology* **75**: 995–1002.

Park S, Kim DH, Yang JH, Lee JY, Lim SH. 2020. Increased flavonol levels in tobacco expressing AcFLS affect flower color and root growth. *International Journal of Molecular Sciences* **21**: 1011.

Pattanaik S, Xie CH, Yuan L. 2008. The interaction domains of the plant Myc-like bHLH transcription factors can regulate the transactivation strength. *Planta* **227**: 707–715.

Pauwels L, Barbero GF, Geerinck J, Tilleman S, Grunewald W, Pérez AC, Chico JM, Bossche RV, Sewell J, Gil E *et al.* 2010. NINJA connects the co-repressor TOPLESS to jasmonate signalling. *Nature* **464**: 788–791.

Pauwels L, Morreel K, De Witte E, Lammertyn F, Van Montagu M, Boerjan W, Inzé D, Goossens A. 2008. Mapping methyl jasmonate-mediated transcriptional reprogramming of metabolism and cell cycle progression in cultured Arabidopsis cells. *Proceedings of the National Academy of Sciences, USA* **105**: 1380–1385.

Peer WA, Murphy AS. 2007. Flavonoids and auxin transport: modulators or regulators? *Trends in Plant Science* **12**: 556–563.

Pérez-Salamó I, Krasauskas J, Gates S, Díaz-Sánchez EK, Devoto A. 2019. An update on core jasmonate signalling networks, physiological scenarios, and health applications. *Annual Plant Reviews Online* **2**: 387–452.

Pierik R, Mommer L, Voesenek LACJ. 2013. Molecular mechanisms of plant competition: neighbour detection and response strategies. *Functional Ecology* **27**: 841–853.

Pradhan M, Pandey P, Gase K, Sharaff M, Singh RK, Sethi A, Baldwin IT, Pandey SP. 2017. Argonaute 8 (AGO8) mediates the elicitation of direct defenses against herbivory. *Plant Physiology* **175**: 927–946.

Rhoades DF, Cates RG. 1976. Toward a general theory of plant antiherbivore chemistry. In: Wallace JW, Mansell RL, eds. *Biochemical interaction between plants and insects*. Boston, MA, USA: Springer US, 168–213.

Schäfer M, Brütting C, Baldwin IT, Kallenbach M. 2016. High-throughput quantification of more than 100 primary- and secondary-metabolites, and phytohormones by a single solid-phase extraction based sample preparation with analysis by UHPLC–HESI–MS/MS. *Plant Methods* **12**: 30.

Schuman MC, Baldwin IT. 2016. The layers of plant responses to insect herbivores. *Annual Review of Entomology* **61**: 373–394.

Schweizer F, Fernández-Calvo P, Zander M, Diez-Diaz M, Fonseca S, Glauser G, Lewsey MG, Ecker JR, Solano R, Reymond P. 2013. Arabidopsis basic helix-loop-helix transcription factors MYC2, MYC3, and MYC4 regulate glucosinolate biosynthesis, insect performance, and feeding behavior. *Plant Cell* **25**: 3117–3132.

Shen Q, Lu X, Yan TX, Fu XQ, Lv ZY, Zhang FY, Pan QF, Wang GF, Sun XF, Tang KX. 2016. The jasmonate-responsive AaMYC2 transcription factor positively regulates artemisinin biosynthesis in *Artemisia annua*. *New Phytologist* **210**: 1269–1281.

Shin J, Heidrich K, Sanchez-Villarreal A, Parker JE, Davis SJ. 2012. TIME FOR COFFEE represses accumulation of the MYC2 transcription factor to provide time-of-day regulation of jasmonate signaling in *Arabidopsis*. *Plant Cell* **24**: 2470–2482.

Shoji T, Hashimoto T. 2011. Tobacco MYC2 regulates jasmonate-inducible nicotine biosynthesis genes directly and by way of the *NIC2*-locus ERF genes. *Plant and Cell Physiology* **52**: 1117–1130.

Soubeyrand E, Johnson TS, Latimer S, Block A, Kim J, Colquhoun TA, Butelli E, Martin C, Wilson MA, Basset GJ. 2018. The peroxidative cleavage of kaempferol contributes to the biosynthesis of the benzenoid moiety of ubiquinone in plants. *Plant Cell* **30**: 2910–2921.

Srivastava AK, Dutta S, Chattopadhyay S. 2019. MYC2 regulates *ARR16*, a component of cytokinin signaling pathways, in Arabidopsis seedling development. *Plant Direct* **3**: e00177.

Staswick PE, Su W, Howell SH. 1992. Methyl jasmonate inhibition of root growth and induction of a leaf protein are decreased in an *Arabidopsis thaliana* mutant. *Proceedings of the National Academy of Sciences, USA* **89**: 6837–6840.

Steppuhn A, Gase K, Krock B, Halitschke R, Baldwin IT. 2004. Nicotine's defensive function in nature. *PLoS Biology* **2**: 1074–1080.

Stork W, Diezel C, Halitschke R, Gális I, Baldwin IT. 2009. An ecological analysis of the herbivory-elicited JA burst and its metabolism: plant memory processes and predictions of the moving target model. *PLoS ONE* **4**: e4697.

Strauss SY, Siemens DH, Decher MB, Mitchell-Olds T. 1999. Ecological costs of plant resistance to herbivores in the currency of pollination. *Evolution* **53**: 1105–1113.

Sui XY, Singh SK, Patra B, Schluttenhofer C, Guo W, Pattanaik S, Yuan L. 2018. Cross-family transcription factor interaction between MYC2 and GBFs modulates terpenoid indole alkaloid biosynthesis. *Journal of Experimental Botany* **69**: 4267–4281.

Sun AQ, Yu B, Zhang Q, Peng Y, Yang J, Sun YH, Qin P, Jia T, Smeekens S, Teng S. 2020. MYC2-activated TRICHOME BIREFRINGENCE-LIKE37 acetylates cell walls and enhances herbivore resistance. *Plant Physiology* **184**: 1083–1096.

Thaler JS, Karban R, Ullman DE, Boege K, Bostock RM. 2002. Cross-talk between jasmonate and salicylate plant defense pathways: effects on several plant parasites. *Oecologia* **131**: 227–235.

Tian B, Pei Y, Huang W, Ding J, Siemann E. 2021. Increasing flavonoid concentrations in root exudates enhance associations between arbuscular mycorrhizal fungi and an invasive plant. *The ISME Journal* **15**: 1919–1930.

Ullmann-Zeunert L, Muck A, Wielsch N, Hufsky F, Stanton MA, Bartram S, Böcker S, Baldwin IT, Groten K, Svatoš A. 2012. Determination of ^{15}N-incorporation into plant proteins and their absolute quantitation: a new tool to study nitrogen flux dynamics and protein pool sizes elicited by plant–herbivore interactions. *Journal of Proteome Research* **11**: 4947–4960.

Wang WJ, Shi XY, Chen DX, Wang FL, Zhang HB. 2020. The *Brassica napus* MYC2 regulates drought tolerance by monitoring stomatal closure. *European Journal of Horticultural Science* **85**: 226–231.

Wasternack C, Kombrink E. 2010. Jasmonates: structural requirements for lipid-derived signals active in plant stress responses and development. *ACS Chemical Biology* **5**: 63–77.

Wei X, Mao L, Wei X, Guan W, Chen R, Luo Z. 2022. AchMYC2 promotes JA-mediated suberin polyphenolic accumulation via the activation of phenylpropanoid metabolism-related genes in the wound healing of kiwifruit (*Actinidia chinensis*). *Postharvest Biology and Technology* **188**: 111896.

Weinhold A, Baldwin IT. 2011. Trichome-derived O-acyl sugars are a first meal for caterpillars that tags them for predation. *Proceedings of the National Academy of Sciences, USA* **108**: 7855–7859.

Woldemariam MG, Dinh ST, Oh Y, Gaquerel E, Baldwin IT, Galis I. 2013. NaMYC2 transcription factor regulates a subset of plant defense responses in *Nicotiana attenuata*. *BMC Plant Biology* **13**: 73.

Xu YH, Liao YC, Lv FF, Zhang Z, Sun PW, Gao ZH, Hu KP, Sui C, Jin Y, Wei JH. 2017. Transcription factor AsMYC2 controls the jasmonate-responsive expression of ASS1 regulating sesquiterpene biosynthesis in *Aquilaria sinensis* (Lour.) Gilg. *Plant and Cell Physiology* **58**: 1924–1933.

Yadav V, Mallappa C, Gangappa SN, Bhatia S, Chattopadhyay S. 2005. A basic helix-loop-helix transcription factor in Arabidopsis, MYC2, acts as a repressor of blue light–mediated photomorphogenic growth. *Plant Cell* **17**: 1953–1966.

Yang Y, Zheng C, Chandrasekaran U, Yu L, Liu C, Pu T, Wang X, Du J, Liu J, Yang F *et al.* 2020. Identification and bioinformatic analysis of the GmDOG1-like family in soybean and investigation of their expression in response to gibberellic acid and abscisic acid. *Plants* **9**: 937.

Yin RH, Han K, Heller W, Albert A, Dobrev PI, Zazimalova E, Schaffner AR. 2014. Kaempferol 3-O-rhamnoside-7-O-rhamnoside is an endogenous

flavonol inhibitor of polar auxin transport in *Arabidopsis* shoots. *New Phytologist* **201**: 466–475.

Zavala JA, Baldwin IT. 2004. Fitness benefits of trypsin proteinase inhibitor expression in *Nicotiana attenuata* are greater than their costs when plants are attacked. *BMC Ecology* **4**: 11.

Zavala JA, Patankar AG, Gase K, Baldwin IT. 2004. Constitutive and inducible trypsin proteinase inhibitor production incurs large fitness costs in *Nicotiana attenuata*. *Proceedings of the National Academy of Sciences, USA* **101**: 1607–1612.

Zhang C, Lei Y, Lu C, Wang L, Wu J. 2020. MYC2, MYC3, and MYC4 function additively in wounding-induced jasmonic acid biosynthesis and catabolism. *Journal of Integrative Plant Biology* **62**: 1159–1175.

Zhang D, Lyu Y, Li H, Tang X, Hu R, Rengel Z, Zhang F, Whalley WR, Davies WJ, Cahill JF Jr *et al.* 2020. Neighbouring plants modify maize root foraging for phosphorus: coupling nutrients and neighbours for improved nutrient-use efficiency. *New Phytologist* **226**: 244–253.

Zhang Q, Xie Z, Zhang R, Xu P, Liu H, Yang H, Doblin MS, Bacic A, Li L. 2018. Blue light regulates secondary cell wall thickening via MYC2/MYC4 activation of the *NST1*-directed transcriptional network in Arabidopsis. *Plant Cell* **30**: 2512–2528.

Zhang Y, Turner JG. 2008. Wound-induced endogenous jasmonates stunt plant growth by inhibiting mitosis. *PLoS ONE* **3**: e3699.

Zhu X, Chen J, Xie Z, Gao J, Ren G, Gao S, Zhou X, Kuai B. 2015. Jasmonic acid promotes degreening via MYC2/3/4- and ANAC019/055/072-mediated regulation of major chlorophyll catabolic genes. *The Plant Journal* **84**: 597–610.

Zhuo MN, Sakuraba Y, Yanagisawa S. 2020. A jasmonate-activated MYC2-Dof2.1-MYC2 transcriptional loop promotes leaf senescence in Arabidopsis. *Plant Cell* **32**: 242–262.

Züst T, Agrawal AA. 2017. Trade-offs between plant growth and defense against insect herbivory: an emerging mechanistic synthesis. *Annual Review of Plant Biology* **68**: 513–534.

Supporting Information

Additional Supporting Information may be found online in the Supporting Information section at the end of the article.

Fig. S1 Experimental design and rationale.

Fig. S2 Timeline of competitive experimental treatments from Figs 4(b) and 5–7.

Fig. S3 irMYC2a/b line construction.

Fig. S4 irMYC2a/b line screening.

Fig. S5 Effects of W + OS elicitation on metabolites in the field (2021).

Fig. S6 Metabolomic analysis in a noncompetitive environment.

Methods S1 Metabolite extraction and analysis.

Table S1 Primers used in this study.

Please note: Wiley is not responsible for the content or functionality of any Supporting Information supplied by the authors. Any queries (other than missing material) should be directed to the *New Phytologist* Central Office.